New Software for Processing of LWD Extra-Deep and Azimuthal Resistivity Data (Russian)

Article · January 2012

DOI: 10.2118/160257-RU

6 authors, including:

Mikhail Sviridov
Baker Hughes Incorporated
14 PUBLICATIONS **29** CITATIONS
SEE PROFILE

Marina Nikitenko
A.A. Trofimuk Institute of Petroleum Geology and Geophysics SB RAS
33 PUBLICATIONS **72** CITATIONS
SEE PROFILE

New Software for Processing of LWD Extradeep-Resistivity and Azimuthal Resistivity Data

M. Sviridov, A. Mosin, Y. Antonov, M. Nikitenko, S. Martakov, Baker Hughes; and
M.B. Rabinovich, BP

Summary

In petroleum exploration, reservoir navigation is used for reaching a productive reservoir and placing the borehole optimally inside the reservoir to maximize production. For proper well placement, it is necessary to calculate in real-time the parameters of the formation we are drilling in and the parameters of formations we are approaching. On the basis of these results, a decision to change the direction of drilling could be made. Modern logging-while-drilling (LWD) extra-deep and azimuthal resistivity tools acquire multicomponent, multispacing, and multifrequency data that provide sufficient information for resolving the surrounding formation parameters. These tools are generally used for reservoir navigation and real-time formation evaluation. However, real-time interpretation software is very often modeled after simplified resistivity models that can be inadequate and lead to incorrect geosteering decisions.

The core of the newly developed software is an inversion algorithm modeled after transversely isotropic layered Earth with an arbitrary number of layers. The following model parameters are determined in real time: horizontal and vertical resistivities and thickness of each layer, formation dip, and azimuth. The inversion algorithm is modeled after the method of the most-probable parameter combination. The algorithm has good performance and excellent convergence because of its enhanced capability of avoiding local minima. This capability enables interpretation of real-time resistivity data, including azimuthal and extra-deep measurements.

A graphical user interface (GUI) was developed to provide an interactive environment for each stage of the resistivity-data-interpretation process: preview of input resistivity logs, initial preprocessing and filtering of raw data, creation of initial guess, running inversion and viewing inversion results, and quality-control indicators. Applications of the developed software will be shown on a series of synthetic examples and field data from the North Sea and Gulf of Mexico (GOM). This newly developed software is currently in use for real-time reservoir navigation and post-well analysis.

Introduction

When the first oil wells were drilled in the mid-1800s, they were vertical and approximately 15 to 30 m deep. Since then, drilling technology advanced significantly, and now a well can be drilled not only several kilometers deep, deviated or horizontal, but following practically any predefined 3D trajectory with high accuracy. Directional drilling has some distinct advantages. For example, a producing area of a horizontal well is much larger than that of a vertical well because oil-saturated reservoirs spread in a lateral direction. Hydrocarbon-saturated layers that are several kilometers away from the drilling rig can be reached by use of directional drilling. This drilling technique becomes even more useful for offshore fields because it enables the use of a stationary rig built onshore or in shallow water.

This paper (SPE 160257) was accepted for presentation at the SPE Russian Oil & Gas Exploration & Production Technical Conference and Exhibition, Moscow, 16–18 October 2012, and revised for publication. Original manuscript received for review 13 May 2013. Revised manuscript received for review 26 January 2013. Paper peer approved 2 January 2014.

AQ10

However, a horizontal or high-angle well is much more difficult to drill, from both engineering and navigation perspectives. Because of the complex well trajectory, a bottomhole assembly (BHA) experiences additional loads, increasing the risk of stick and slip and of wellbore instability. Drilling near dangerous objects such as salt domes or overpressured layers can also increase risk. In addition, the primary goal of landing a well within a hydrocarbon-bearing layer and steering inside it is a very complicated task. To better understand the geological situation surrounding a well, service companies perform a series of formation-evaluation measurements (LWD), core sampling, and formation testing. Accurate evaluation of surrounding and approaching formations is needed for real-time adjustments of a borehole trajectory during drilling to prevent unwanted events such as exiting a reservoir layer or approaching an oil/water contact.

A propagation resistivity tool has one of the largest depths of investigation (DOIs) among all LWD measurements. Neutron, density, and gamma ray measurements are usually used to define the rock properties within a few inches of the borehole, whereas parameters of more remote areas are defined mostly by propagation resistivity measurements. It should be mentioned that the DOI of resistivity propagation tools can be increased by increasing the distance between transmitter and receiver and by decreasing the transmitter frequency range, but this increase in DOI is limited because of additional power supply restriction.

Existing propagation LWD tools could be divided into two groups: deep-resistivity tools that are sensitive up to 3 to 5 m from the well and extradeep-resistivity tools that are sensitive up to 10 m or more. Different definitions of the DOI and depth of detection for propagation resistivity tools are discussed in detail in previous publications (Rabinovich et al. 2011).

Resistivity propagation tools are usually used for numerous purposes while navigating a well:

- Landing a well: entering a reservoir at a certain angle to optimize the well path for the subsequent horizontal drilling and completion.
- Geosteering in a reservoir: performing real-time well-path adjustment to optimize the position within the reservoir and to minimize the risks associated with exiting the productive layer and approaching oil/water or oil/gas contacts.
- Searching for a reservoir: detecting additional reservoirs that are screened by conductive shale. Sometimes, there is a need to find an additional hydrocarbon-bearing layer because the current layer might be pinching out or its properties (porosity and/or permeability) deteriorate.

Propagation resistivity tools with different DOIs can be used during different drilling stages. On occasion, a combination of tools is needed. For example, to avoid drilling into the roof, a conventional deep-resistivity tool is sufficient, whereas for aggressive landing (using relatively low angles), the extradeep-resistivity tool is preferred. A combination of deep and extradeep tools is recommended to detect an extra reservoir screened by a conductive layer. In the latter case, shallower measurements can be used to define the parameters of a current layer, and then a combination of deep and extradeep measurements can be used to define boundaries and parameters of remote layers.

During the past decade, increasing reservoir complexity and more-challenging tasks addressed during reservoir navigation led

Fig. 1—Schematic of an extradeep-resistivity tool.

to the development and introduction of new propagation resistivity tools such as azimuthal and extradeep-resistivity tools. These tools acquire multifrequency, multicomponent, and multispacing measurements that are essentially nonlinear with respect to formation parameters. More-sophisticated multiparametric inversion algorithms are required to combine all these measurements into one processing algorithm and accurately resolve the formation parameters. Mathematically, this inversion is nonlinear and ill posed, which means the solution could be nonunique and difficult to find. Advanced optimization techniques, including special regularization, are needed to resolve the ambiguity and find a solution approximating the reality to the best of our abilities. The necessity of providing real-time solutions places additional requirements on the inversion algorithm. Results must be accurate and reliable, and the recovered model must be consistent with a priori information. A solution must be obtained in real time so that a timely decision to change a well path can be made.

In this paper we describe an efficient multiparametric inversion algorithm and present a newly developed multicomponent-while-drilling (MCWD) software for reservoir-navigation and formation-evaluation applications. The MCWD software can perform real-time processing of any combination of the omnidirectional, azimuthal, and extradeep LWD resistivity measurements. The algorithm is based on a 1D anisotropic layered model. Any parameters of this model, including layer boundary positions relative to a borehole trajectory, can be recovered. The developed software has been used for real-time geosteering applications as well as during post-drill analysis to provide accurate estimations of formation parameters.

LWD Azimuthal and Extradeep-Resistivity Measurements

When LWD propagation resistivity tools were introduced in the 1980s, they were used in typical formation-evaluation applications such as calculation of water saturation, similar to conventional wireline induction tools. Unlike wireline induction logging tools, LWD measurements are performed at higher frequencies to overcome the effects of a metal tool body and to boost the signal strength coming from slotted antennas. In addition, relative measurements of phase difference and attenuation (amplitude ratio) are made instead of real and imaginary parts of an electromagnetic field. These relative measurements provide additional rejection of the signal coming from metal collar and borehole and eliminate the need for transmitter/receiver synchronization.

In the late 1990s, with the rapid adoption of horizontal drilling, LWD resistivity measurements became a principal measurement for reservoir navigation. The DOI of the LWD resistivity tools was significantly larger than that of other LWD tools (such as gamma ray, nuclear, acoustic, or nuclear magnetic resonance), making LWD resistivity tools much more attractive for such applications. Today, the primary goal of the use of LWD tools is to land a well, steer it inside the reservoir, and (if necessary) find an additional reservoir. These tasks may have different depth scales and require tools with different DOI.

To satisfy this demand, deeper-reading LWD resistivity tools were developed. First-generation tools appeared in 2003 and 2004 (Seydoux et al. 2003; Helgesen et al. 2004). These tools used transmitter/receiver spacing 10 to 20 times longer and operating frequencies 10 to 20 times lower to achieve the required DOI. For example, an extradeep-resistivity tool (Helgesen et al. 2004) in **Fig. 1** measures the phase difference and attenuation at two receiver antennas 12 and 17 m from the transmitter at operating frequencies of 20 and 50 kHz.

Because of the axial symmetry of the transmitter and receiver coils around the tool axis, LWD resistivity tools lacked azimuthal sensitivity. Although azimuthal sensitivity was not important for typical formation-evaluation applications, for many reservoir-navigation applications this capability became critical. As shown in **Fig. 2,** because of the lack of azimuthal sensitivity (the tool responses in both cases are identical) an operator cannot make an

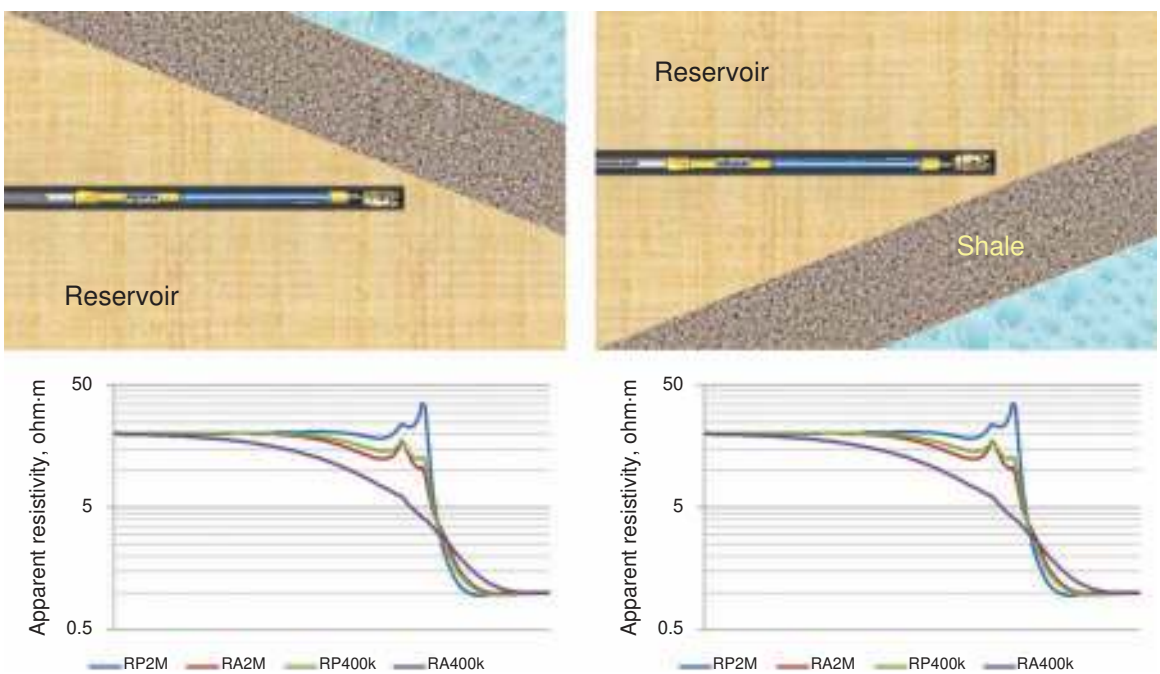

Fig. 2—Approaching a shale layer with an omnidirectional LWD resistivity tool. In the left picture, the BHA approaches the shale layer from the bottom, whereas in the right picture it approaches from the top. The bottom plots show responses of the omnidirectional propagation resistivity tool. These identical responses illustrate the lack of azimuthal sensitivity of conventional omnidirectional tools.

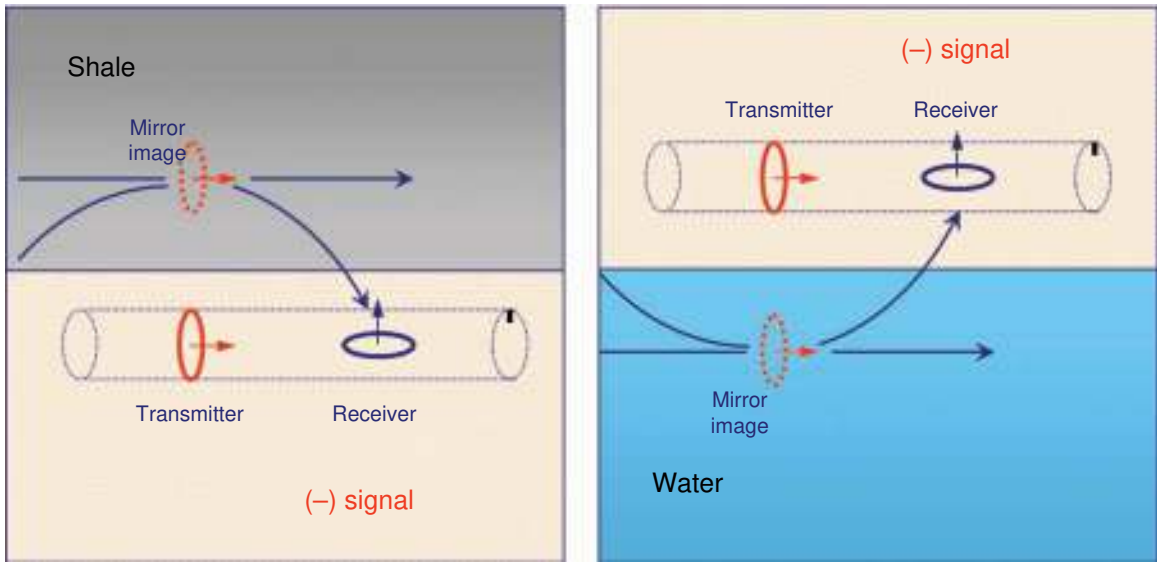

Fig. 3—Azimuthal sensitivity of a cross-component signal to a conductive layer. The sign of the signal is different depending on whether the conductive bed is above or below the tool.

informed decision to drill up or down to avoid exiting the reservoir unless some preconception of the formation model is used (shale roof above or a water contact below).

To address the demand for azimuthal sensitivity, the service companies recently introduced a new generation of azimuthal resistivity tools that used tilted or orthogonal coils to measure cross-component signals. **Fig. 3** shows the azimuthal sensitivity of the so-called ZX signal to a conductive bed. The sign of the signal is different depending on whether the conductive bed is above or below the tool.

A schematic view of an azimuthal resistivity tool is presented in **Fig. 4** (Wang et al. 2007). The tool consists of four coaxial transmitting coils—T1, T2, T3, T4—with a magnetic moment oriented along the z-axis; two coaxial receiving coils—R1, R2—with a moment oriented along the z-axis; and two orthogonal receiving coils—R3, R4—with a moment oriented along the x-axis. We will call ZZ a signal measured by receiving coils R1 and R2, and ZX a signal measured by R3 and R4. The tool operates on 400-kHz and 2-MHz frequencies, measuring the phase difference and attenuation for ZZ signals, and the real and imaginary part of induced voltage for ZX signals (Fang et al. 2008).

Usually, LWD measurements are made while the BHA is rotating. The azimuthal resistivity tool acquires ZX signals in 16 sectors, as shown in **Fig. 5.** ZX response in layered formation could be described with a curve $A\cdot\cos(\phi–\phi_0)$, and it enables significant noise reduction by use of least-squares cosine fitting filtering. As the tool is rotating, ZX signal extrema $\phi=\phi_0$ and $\phi=\phi_0+180°$ are reached for a tool position when an x-coil moment is orthogonal to the boundary. When the moment of the x-coil is parallel to the boundary, the tool reading is zero. Curve maximum $\phi=\phi_0$ reflects the direction to the nearest conductive layer, as shown in Fig. 5.

Simple visual-interpretation techniques became practically useless with the introduction of the multicomponent and extra-deep propagation measurements. The only solution to the problem of processing of multiple measurements with different DOI and different sensitivity to various formation parameters is the use of multiparametric inversion based on adequate formation-model representation and corresponding fast-forward modeling.

MCWD Inversion Software

In simple scenarios of proactive geosteering, such as controlling a distance to a remote bed, simple interpretation approaches are commonly used and are quite successful. For example, visual reduction in a low-frequency attenuation resistivity curve (RA400k signal) could indicate an approaching conductive layer. Simple depth-by-depth inversion for the distance to bed (D2B) and the resistivity of the remote layer, based on two or three measurements including azimuthal resistivity, can provide reliable quantitative evaluation. This approach is proved to work well when only one bed boundary interface is within the range of the tool's DOI.

Employing the extradeep-resistivity tool with significantly larger DOI requires that several boundaries must be taken into account. Also, its signal behavior becomes too complex for visual or simplistic interpretation. A more-advanced inversion algorithm must be applied when extradeep tools are used for steering. This algorithm must be modeled after a multiparametric inversion and should be able to describe complex models with multiple layers and combine various measurements to resolve those parameters.

Mathematically, this inversion is nonlinear and ill posed, indicating that the solution could be nonunique and difficult to find. Advanced optimization techniques including special regularization are needed to resolve the ambiguity and find a solution approximating real formations in the best possible way. The necessity of providing real-time solutions brings additional requirements to the inversion algorithm for accuracy, reliability, and speed.

For this purpose, we developed an efficient inversion algorithm and included it in a user-friendly software package that performs real-time processing of any combination of omnidirectional, azimuthal, and extradeep LWD resistivity measurements. The algorithm is based on the 1D anisotropic layered model and can recover any parameter of this model, including layer boundary positions relative to a borehole trajectory. In this section, we discuss the locally 1D layered model with arbitrary number of layers, which enables the use of a fast-forward modeling solver and simultaneous accounting for different DOIs of various measurements; efficient nonlinear optimization that accommodates

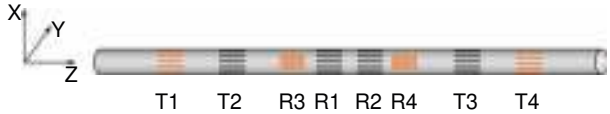

Fig. 4—Schematic of an azimuthal resistivity tool.

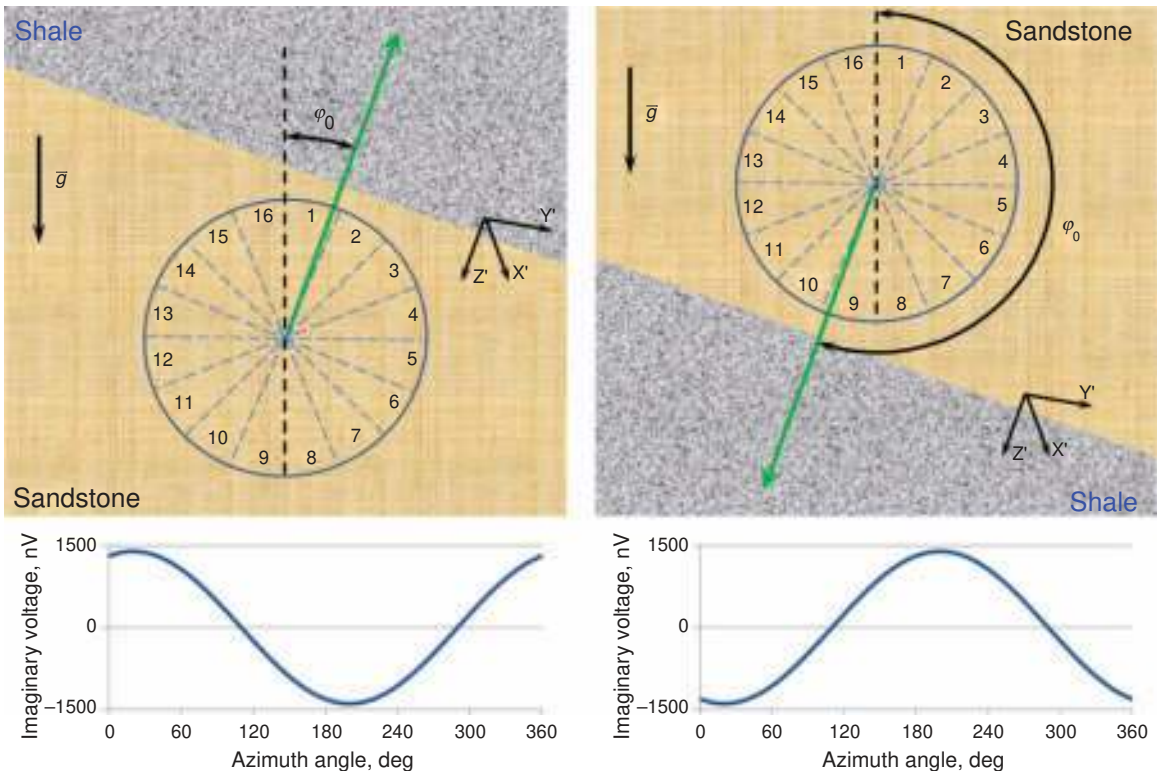

Fig. 5—ZX cross-component measurements while approaching a shale formation. As the drillstring is rotating, the azimuthal resistivity tool acquires ZX signals in 16 sectors at each logging depth. When the *x*-coil is orthogonal to the boundary (the magnetic moment of *x*-coil is parallel to the boundary), the ZX reading is zero. Curve maximum at $\phi=\phi_0$ indicates the direction to the nearest conductive layer.

multiple unknowns, contrary to the look-up table approach; global minimum search and problems of inversion ambiguity; and GUI.

Formation Model. Let us assume that layer thicknesses vary insignificantly along the interval of interest and that the medium does not pinch out or include faults or other 3D geological features—otherwise, the interval should be split into several smaller pieces. In this scenario, the formation model could be approximated as a 1D horizontally layered model with a local coordinate system $x,'y,'z'$, where z' is oriented normally to boundaries and the x'-axis is oriented along the tool projection to the plane that is perpendicular to z' (Fig. 5).

The majority of nonlinear inversion algorithms call a forward problem solver thousands of times during the inversion until the optimal solution is found. This reality dictates very high performance requirements for the forward problem solver. The MCWD software uses a specially developed fast solver that calculates an electromagnetic field for a layer-cake model, neglecting borehole and invasion effects, which are reasonable assumptions for LWD applications.

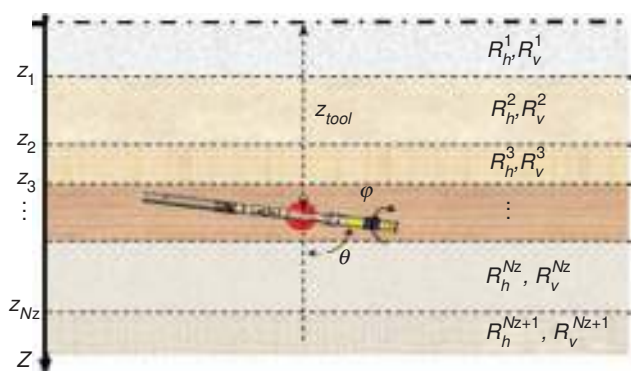

Fig. 6—1D horizontally layered model. The parameters of the model are horizontal and vertical resistivities, coordinates of layer boundaries, relative dip, and rotation angle.

There are many known implementations of 1D forward solution based on look-up tables, Anderson's filters, or explicit quadrature formulas for integration with Bessel functions. They usually vary in speed and in accuracy. Our implementation of the semianalytical (we called our solution semianalytical because the integrand function in the Fourier integral is calculated analytically as the solution of a nonlinear-equation system, whereas the computation of the Fourier integral is performed numerically using the Gaussian quadrature) forward solver features the following:

- Computes all magnetic-field components for all transmitter/receiver spacings and tool positions simultaneously
- Allows controlled accuracy of integration with Bessel functions
- Employs real axis or complex domain integration path, depending on well trajectory and formation contrasts
- Calculates Jacobian simultaneously with magnetic fields with almost no additional computational cost
- Optimizes speed vs. accuracy for each tool in the library

Each layer is described by three parameters: horizontal resistivity (R_h), vertical resistivity (R_v), and a coordinate of a bottom boundary (Z) **(Fig. 6).** The software described in this paper accounts for a different anisotropy coefficient (R_v/R_h) for each layer. A tool position is described by its z-coordinate, a dip angle (θ) relative to the layer bedding plane, and a tool rotation angle (ϕ). For the implementation of the inversion algorithm, it is more convenient to consider the tool position as fixed and search for the distances to the boundaries. During inversion, each parameter could be assumed to be known and accordingly predefined and fixed, or unknown and determined by inversion.

A well trajectory is required as an input to the software. The well trajectory is described by the measured-depth (MD) distance along the well and inclination ($\theta_{\text{tool}}^{\text{abs}}$) and azimuth ($\phi_{\text{tool}}^{\text{abs}}$) angles at each depth. Thus, if we know the tool orientation relative to the layer boundary (angles $\theta_{\text{tool}}^{\text{local}}$ and $\phi_{\text{tool}}^{\text{local}}$), an absolute orientation of the layer could be calculated **(Fig. 7).**

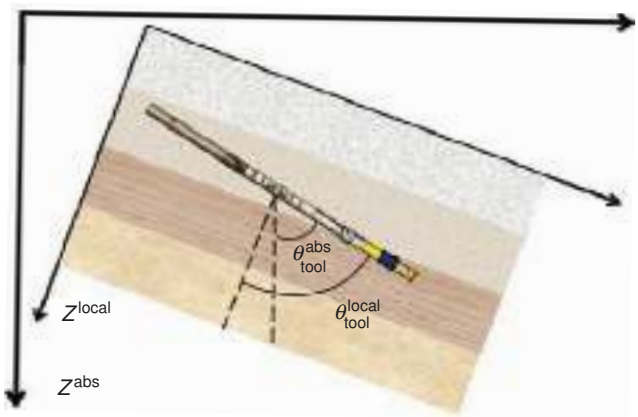

Fig. 7—Absolute and local coordinate systems and corresponding angles.

Inversion Algorithm. The inversion algorithm is modeled after the method of the most-probable parameter combination (Verlan and Sizikov 1986), which is a combination of Tikhonov's regularization and the method of Kalman's filter (Tikhonov and Arsenin 1979; Yanovskaya and Porokhova 1983). The aim of the most-probable parameter combination method is finding the minimum of the following objective function (OF):

$$OF = \Delta F^T C_F^{-1} \Delta F + \alpha^2 \Delta X^T C_X^{-1} \Delta X + P^T P. \quad \ldots\ldots\ldots \quad (1)$$

Here, ΔF is the difference between simulated and measured signals; ΔX is the difference between recovered and expected model parameters; and vector P consists of penalty functions responsible for parameter constraints. The constant α is a regularization parameter that can be chosen by the method of quasioptimal choice (Yanovskaya and Porokhova 1983) or the method of matching by independent measurement subsets (Stone 1974), and C_X and C_F are covariance matrices of model parameters and measured signals, respectively.

The first term in Eq. 1 ensures reduction of the data misfit. The second term (regularization term) stabilizes the convergence process by pushing the solution toward the expected model. The third term keeps parameters confined inside the predefined domain. In our realization of this method, the model parameters used in the inversion are transformed to provide the simplest form of the cost function. For example, along with the dip angle θ, the following parameters are used in inversion: the logarithms of layer resistivities, the anisotropy ratios (instead of R_h and R_v), and the layer thicknesses (instead of bed-boundary coordinates). Expected values and parameter constraints are usually chosen depending on available a priori information about the formation structure, and also are determined by the qualitative analysis of the data. Indeed, the direction to the nearest conductive layer according to azimuthal signals and behavior of apparent resistivity curves with different DOI and their separation along the well can be used for the construction of the initial inversion model. Certain techniques of expected-values definition are outside the scope of this paper. Here, we want to stress that expected values play an important role in inversion and the developed software allows the user to influence their choice.

Two optimization methods are used in the new software. The first is the box complex method (Gill and Murrey 1977), a modification of the Nelder-Mead simplex approach (Himmelblau 1975), is the first method used. In the Nelder-Mead method, an n-dimensional simplex used to find the minimum of the n-parameter function can be degenerated near the area with penalty restrictions. The box complex method contains m points, where $n+1 < m \leq 2n+1$. Additional points enable the box method to work in the full-dimension parameter domain. The disadvantage of this method is the low rate of convergence. However, this method has an indispensable feature: It scans the parameter domain more reliably when a search for the global minimum is needed.

The second method is the descent method, which is the modification of the Levenberg-Marquardt method (Dennis and Schnabel 1988). The quadratic model is constructed by the Gauss-Newton method. In this implementation, the direction and length of steps are chosen according to the rule called the "model-trust region" (Moré and Sorensen 1983). The current method has good performance and a high rate of convergence. Moreover, it is consistent in the case of a singular Jacobian matrix and it does not make big steps, even in the case of very nonlinear models.

The descent method is the default option in the inversion algorithm because of its high performance, but there is an option to switch to the box complex method when the speed is not critical (for example, in case of post-drill data analysis or research tasks) and/or when global scanning of the parameter domain is important.

Global Minimum Search and Ambiguity. There is a broad variety of optimization methods that can find the local minimum of a function. They use different algorithms and vary in performance, but all typically guarantee convergence within a certain time frame (e.g., the local optimization technique we previously described, the descent method). There are several popular global optimization techniques known from the literature, but they are usually inefficient and do not guarantee the convergence in reasonable time. Two of them are commonly used in practical applications: (1) the method of a full scanning in the parameter domain with a step size for each parameter that guarantees the required accuracy, which always leads to the global minimum but may have an enormous time cost, and (2) the Monte Carlo method, which generates several random points over predefined parameter domain, calculates the value of the objective function for each of them, and then considers the smallest as a global minimum.

Carrying out the inversion, we are interested in finding either the global minimum or a local solution that is sufficiently close to the global minimum or the best local minimum found during a given amount of computational time. To achieve that, the MCWD software uses an effective heuristic algorithm that combines the advantages of both global and local optimization techniques and can be referred to the class of two-phase methods of global optimization (Pardalos and Romeijn 2002). Namely, starting points for a certain number of local optimizations are chosen randomly to perform a preliminary scanning of a parameter domain, so the majority of easily found (distinct) local minima (often one of them is coincident with the global minimum) in the parameter domain will be checked at the initial iterations. Information about previously scanned trajectories is stored in memory, and is taken into account to generate each subsequent starting point for the local optimization. The algorithm stops when the required misfit level is obtained or the maximum number of iterations is reached. This algorithm can be easily programmed for parallel central processing units, which is critical for real-time applications. Note that the strategy of starting from the point that accounts for the minimal cost-function value does not guarantee success in the global search. The reason is that an optimization trajectory starting from a "good" point can become stuck in a local minimum, whereas a trajectory from a "bad" point can finally converge to the global minimum.

Let us illustrate a global minimum search with the following examples. When the distance to bed (D2B) is the only parameter to be determined, the whole inversion process may be illustrated in **Fig. 8.** We assume that the layer resistivities are known and that the tool is in a resistive layer. In this scenario, the D2B value could be uniquely determined from only one ZX signal (ImV400k): 170 nV of measured ZX signal corresponds to 2 m of D2B. The accuracy of this inversion would depend only on the ZX signal measurement accuracy. If we know, for example, that the 170-nV signal is measured with a noise/uncertainty of ± 20 nV, we can tell that the uncertainty in D2B will be ± 0.1 m (D2B is between 1.9 and 2.1 m).

Typically, the topology of the objective function becomes more complex (it includes multiple local minima) and the search

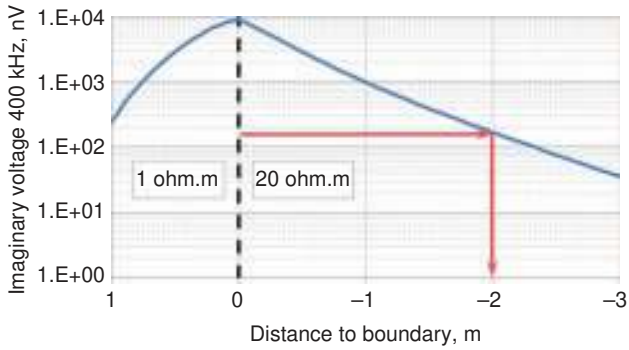

Fig. 8—Determining D2B in a model with two layers by use of the ZX signal. The *x*-axis presents the distance to the boundary, whereas the boundary itself is at 0. The *y*-axis shows an imaginary part of ZX voltage in nV for the two-layer model with resistivities 1 and 20 Ω·m. If these resistivities are known and the tool is in the resistive layer, the D2B value could be uniquely determined from the ZX signal; for example, 170 nV of measured ZX signal corresponds to 2 m of D2B. The only uncertainty in the result is related to the accuracy of the ZX signal measurement.

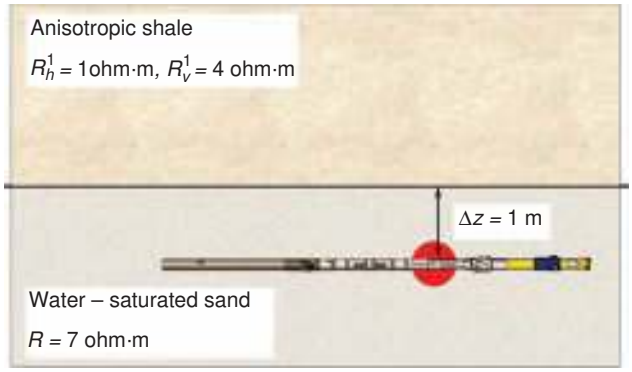

Fig. 9—Two-layered model with two unknowns: distance to bed and horizontal resistivity of the upper layer. We assume that the resistivity of the water-saturated sand (7 Ω·m) and anisotropy ratio (4:1) of the upper layer are known.

for a global minimum becomes more difficult when the number of unknown model parameters increases. We will illustrate this with an example of a two-layer model. Imagine the tool is moving up through a layer with resistivity of 7 Ω·m and is approaching an anisotropic layer with a horizontal resistivity of 1 Ω·m and vertical resistivity of 4 Ω·m **(Fig. 9).** Let us consider a point where the tool is 1 m away from the boundary and the relative dip is 91°. For this case, we assume we know the parameters of the layer in which we are drilling, the anisotropy ratio of a layer above the tool, and the dip angle. In this case, we must determine D2B and horizontal resistivity of the upper layer. Because we need to determine two unknown parameters, one signal is not enough in this case. Let us use three signals: two ZZ signals and one ZX signal. Contrary to the previous example, a unique pair of unknown parameters could not be visually determined, so there is a need to apply an inversion algorithm. However, the topology of the minimized objective function is complicated, as shown in **Fig. 10,** and there is no unique solution. Regions that produce a misfit smaller than the required threshold in the MCWD inversion include a number of equivalent solutions. We show starting vectors of model parameters with green points. Red points represent the solution found from each starting point. The true global minimum is shown with a red star.

As shown in Fig. 10, a solution of the inverse problem may be nonunique. In the majority of cases, it is caused by the lack of independent measurements, low sensitivity of signals, measurement noise, and insufficient a priori information. In this particular case, the use of a more-sensitive 2-MHz ZX signal instead of one of the ZZ signals or a priori information about resistivity of the upper layer would dramatically reduce the ambiguity. In the right panel of Fig. 10, we show that the ambiguity region is significantly reduced when the 2-MHz ZX signal (ImV2M) is used instead of 400-kHz ZZ attenuation. To address these issues, the developed MCWD inversion software enables the processing of any combination of acquired measurements, as well as incorporation of a priori information.

In the last two examples, the relative dip was considered to be known. Numerical modeling studies and application of different inversion algorithms on the field data showed that D2B can be determined from conventional LWD resistivity measurements with

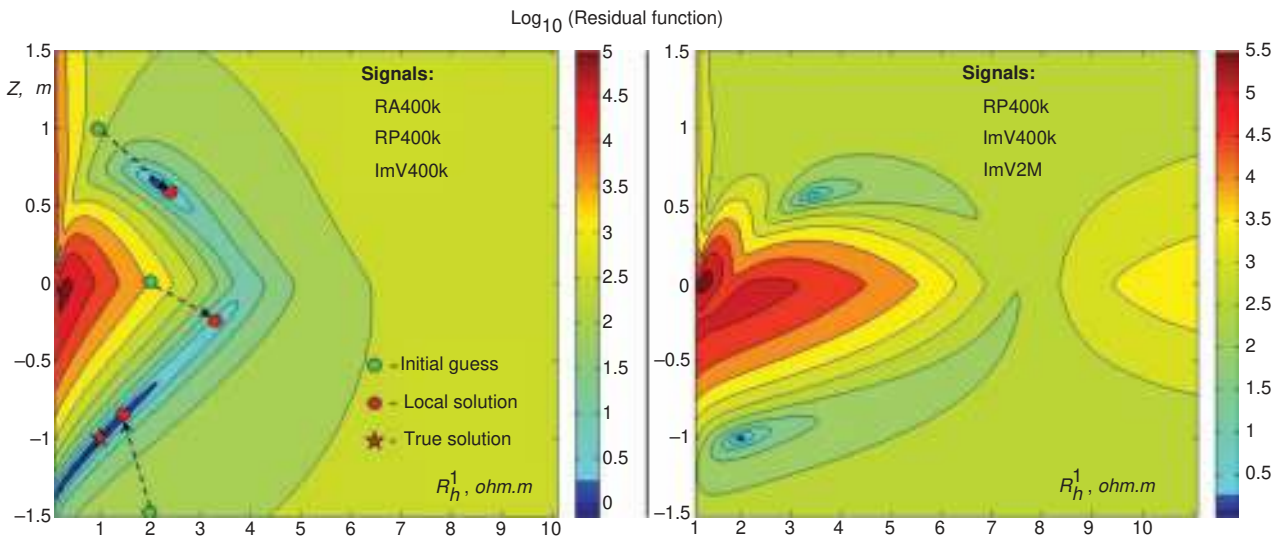

Fig. 10—Minimized-objective-function topology. The corresponding model is shown in Fig. 9. The objective function in χ^2-norm is presented as a color-coded map. The *x*-axis depicts horizontal resistivity of the upper layer, whereas the *y*-axis presents the distance to bed. Light and dark blue colors show the regions that produce a misfit smaller than the required threshold in the MCWD inversion. Initial model parameters are shown as green points. Red points represent the solution found from each starting point. The true global minimum is shown with a red star. In the left picture, the objective function is constructed on the basis of the two ZZ signals (RA400k and RP400k) and the single ZX signal (ImV400k). In the right picture, the objective function is constructed on the basis of the single ZZ signal (RP400k) and the two ZX signals (ImV400k and ImV2M). The ambiguity region in the right picture is significantly less than the ambiguity region in the left picture.

ID: jaganm Time: 20:11 I Path: S:/3B2/REE#/Vol00000/140009/APPFile/SA-REE#140009

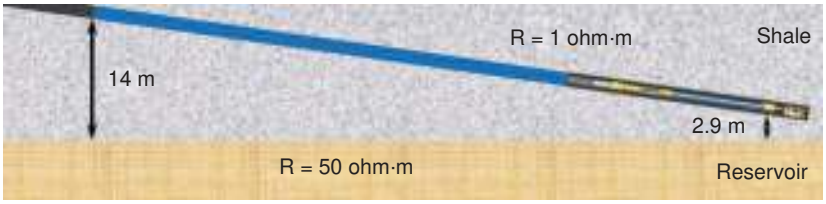

Fig. 11—Model used in Synthetic Example 1. Landing of horizontal section of the well started in shale 14-m TVD above the expected productive sand. Both azimuthal and extradeep-resistivity tools are used for reservoir navigation. Resistivity of shale is 1 Ω·m and of the hydrocarbon-bearing sand is 50 Ω·m. A section of the well shown in blue is drilled at a constant dip angle of 82°. Corresponding distances to the reservoir in TVD at the beginning and at the end of this section are 14 and 2.9 m, respectively.

sufficient accuracy when the relative dip is known within ± 5°. Some commercial geosteering inversion codes always consider that the tool is parallel to the formation bedding (i.e., 90° relative dip). However, for the ZX measurements of an azimuthal resistivity tool or extradeep-resistivity-tool measurements, such errors or assumptions about relative dip may generate large errors in D2B. To avoid these concerns, we often run MCWD inversion with the dip as an unknown parameter when the previously discussed measurements are used.

The main purpose of the developed MCWD software package is advanced data processing and interpretation. Various situations arising during real-time reservoir navigation require thorough analysis that could not always be performed automatically. The developed software provides additional capabilities compared with standard automatic point-by-point real-time interpretation. First, an interpretation model may include an arbitrary number of layers, which is critical especially for the interpretation of a deep-reading tool and for detecting remote objects. Second, an inversion can be made for any combination of measurements that increases the certainty of the final result. Third, the MCWD software allows setting constraints for each parameter according to the operating geologist's expectations. This a priori information improves the convergence speed and guarantees consistency with the expected geological model.

Specifying the number of layers in the model on the basis of a priori knowledge of geology reduces the ambiguity of inversion and improves its convergence. In some scenarios, such as landing a well from a thick shale layer into a reservoir or steering in a thick sand, the use of a two-layer model could be a reasonable assumption. In other cases, it will not work and a general inversion workflow should include processing of several models with different complexity. Usually it starts with an attempt to use the simplest model with the minimal number of layers and unknown parameters, and stops if the reasonable misfit is achieved. When a simple model cannot explain the data, another layer or unknown parameter is added and this process continues until the measured data are reasonably approximated. In case studies discussed later, this approach sometimes results in abrupt changes in reconstructed models observed on adjacent intervals.

One more feature of the software is the "log generation" mode that enables a study of simulated tool responses in typical geologic situations. This option also helps in tool design through study of tool response sensitivity and its optimization in different environments. MCWD can also be used for prejob modeling if information from pilot wells is available.

GUI. To take full advantage of such sophisticated data-processing software, it is critical to have an easy and convenient way to adjust its control parameters and view the results. For this purpose, we have developed a GUI that controls all the features of the MCWD software in a user-friendly manner. The newly developed GUI extends capabilities of current reservoir-navigation service with a flexible and convenient tool for advanced processing of LWD resistivity data. The MCWD GUI is applied in more-complicated log sections where standard automatic D2B inversion could produce inconsistent results. To support real-time reservoir navigation, a direct connection to a rig database is implemented with wellsite information transfer standard markup language. Currently, MCWD GUI supports the following functions:

- Displaying the measured data (apparent resistivities or measured phases, attenuations, and voltages) and their filtering
- Preprocessing of data (Pustilnik 1968), including estimation of and setting the signals' noise level
- Selecting data, including selection of the logging interval and a combination of measurements for inversion
- Setting a priori information for formation parameters
- Executing MCWD inversion and monitoring its progress
- Displaying and analyzing the resulting formation parameters, including uncertainty analysis
- Displaying data misfit in different norms (inversion quality control)
- Saving and loading previous inversion configuration and results
- Generating synthetic logs and performing resolution analysis

In real-time reservoir navigation and in predrill or post-drill analysis, it is critical that the operating geologist's knowledge and expectations on formation parameters and on their constraints are properly taken into account. The MCWD GUI, with its interactive and flexible control of all the multiple inversion features, ensures this.

Applications of MCWD Inversion

In this section, we present three synthetic examples and two case studies, with one from the North Sea and another from the GOM. In the first synthetic example, we simulate the reservoir-navigation scenario of landing a well. In the second example, we model the scenario of steering a well within a relatively thin reservoir. In the third example, we investigate the detection of a remote layer. In the first two cases, we consider interpretation of the azimuthal resistivity data alone and in combination with extradeep resistivity. In the third example, we evaluate only the combination of two tools. The North Sea case study illustrates the application of the MCWD inversion for identification of a shale injectile. The GOM case study demonstrates the benefits of the MCWD inversion in identifying a thin shale layer while geosteering within the reservoir. In all examples, the high quality of inversion processing is confirmed by excellent reconstruction of the measured signals. In all the synthetic examples, the data were contaminated with 2% relative noise and an absolute noise dependent on signal type (0.01 dB for all attenuation signals, 0.1° for all phase signals, and 10 nV for ZX voltage).

Synthetic Example 1: Landing a Well. Let us consider the following landing scenario **(Fig. 11):** The casing is set in the shale 14-m true vertical depth (TVD) above the expected productive sand, and reservoir navigation is carried out by use of azimuthal and extradeep-resistivity tools to land a horizontal section into reservoir. In this situation, it is very important to detect the approaching reservoir boundary as soon as possible and make a decision to build up a drilling angle for a smooth entry into the reservoir. Otherwise, the sand could be passed through because of the dogleg restriction, and hundreds of feet of productive zone will be missed. That is why the use of the extradeep-resistivity measurements in this scenario is critical. Shallower signals of the azimuthal resistivity tool can be used for accurate estimation of

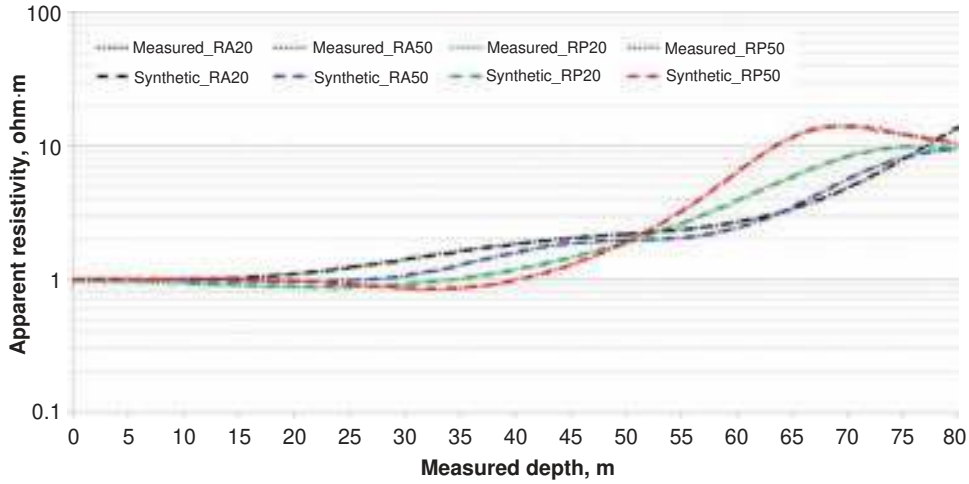

Fig. 12—Measured and synthetic signals of the extradeep-resistivity tool for the landing scenario. Measured data are shown with dotted lines; calculated data for the model recovered by the inversion are shown with dashed lines. Close data fit obtained for the entire interval confirms the high quality of inversion. Beginning at 10-m MD, an indication of the approaching resistive layer is seen in the extradeep readings.

shale resistivity and for reducing ambiguity of extradeep-resistivity data.

For simplicity, we consider drilling at a constant dip angle of 82°. We look at the interval 0- to 80-m MD along the borehole (highlighted blue segment of borehole in Fig. 11). The signals for extradeep and azimuthal resistivity tools for this interval are shown as dotted lines in **Figs. 12 and 13,** respectively. In the beginning of this interval (0- to 10-m MD), all resistivity readings are constants: ZZ signals for both extradeep and azimuthal resistivity tools read 1 Ω·m, which is the resistivity of shale, and the ZX signal is zero. Beginning at 10-m MD, extradeep signals "sense" the approaching resistive layer. Fig. 12 shows that they deviate from the constant value.

The MCWD inversion results are presented in **Figs. 14a and 14b.** The 80-m interval was split into 5-m windows, and in each window an independent inversion processing was carried out. The recovered resistivities in Ω·m are presented as numbers for each window. The difference in results presented in Figs. 14a and 14b is caused by different a priori information used in these inversions. The a priori information, initial model, and used signals are presented in **Tables 1 and 2.** In the first case, we specified that the expected resistivity of the second layer is 1 Ω·m, and in the second case the expected value was set to 80 Ω·m. We can see the uncertainty in the recovered resistivity of the approaching layer and how it converges to the true value when the BHA approaches the interface. The reconstructed signals for both extradeep and azimuthal resistivity tools for the model shown in Fig. 14a are depicted as dashed lines in Figs. 12 and 13, and they practically coincide with the input signals, confirming the quality of the inversion processing. The MCWD inversion results in Figs. 14a and 14b illustrate that the extradeep propagation tool detects the boundary of the approaching resistive layer, starting at the distance of approximately 12 m, and the inversion can resolve the distance to this boundary within an error range of approximately 1 m. At the same time, the resistivity of the approaching sand is not accurately recovered when the tools are distant, but the accuracy improves when the tools approach the boundary. We showed here that a priori information about approaching objects—in this case the resistivity of the remote layer—can be very useful and can regularize inversion and improve its accuracy.

The inversion results for the landing scenario when only the azimuthal resistivity tool is used are depicted in **Fig. 15,** and the corresponding measured and synthetic data are presented in **Fig. 16.** The a priori information, initial model, and used signals are

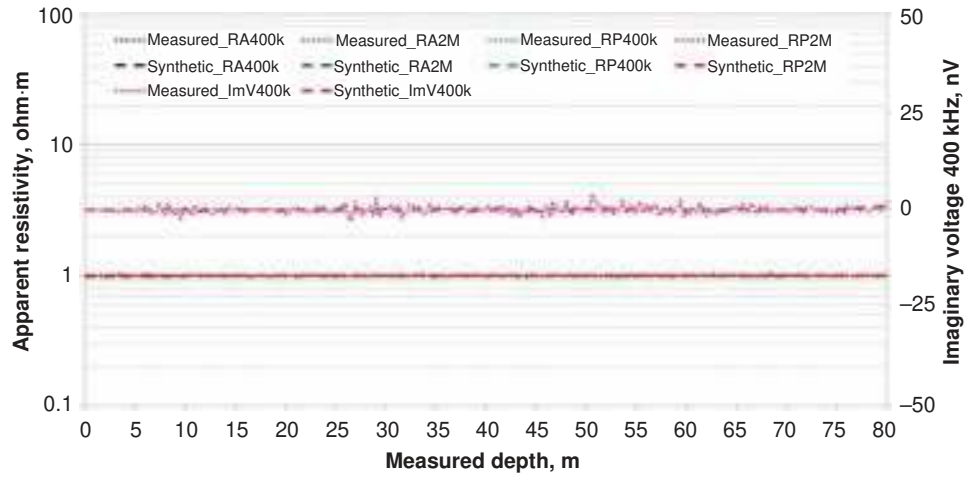

Fig. 13—Measured and synthetic signals of the azimuthal resistivity tool for the landing scenario. Measured data are shown with dotted lines; calculated data for the model recovered by the inversion are shown with dashed lines. Close data fit obtained for the entire interval confirms the high quality of inversion. For this interval, azimuthal resistivity data do not show any indications of the approaching sand: ZZ components read 1 Ω·m, which is the resistivity of shale, and the ZX signal is zero. The approaching boundary is beyond the azimuthal resistivity tool's depth of detection.

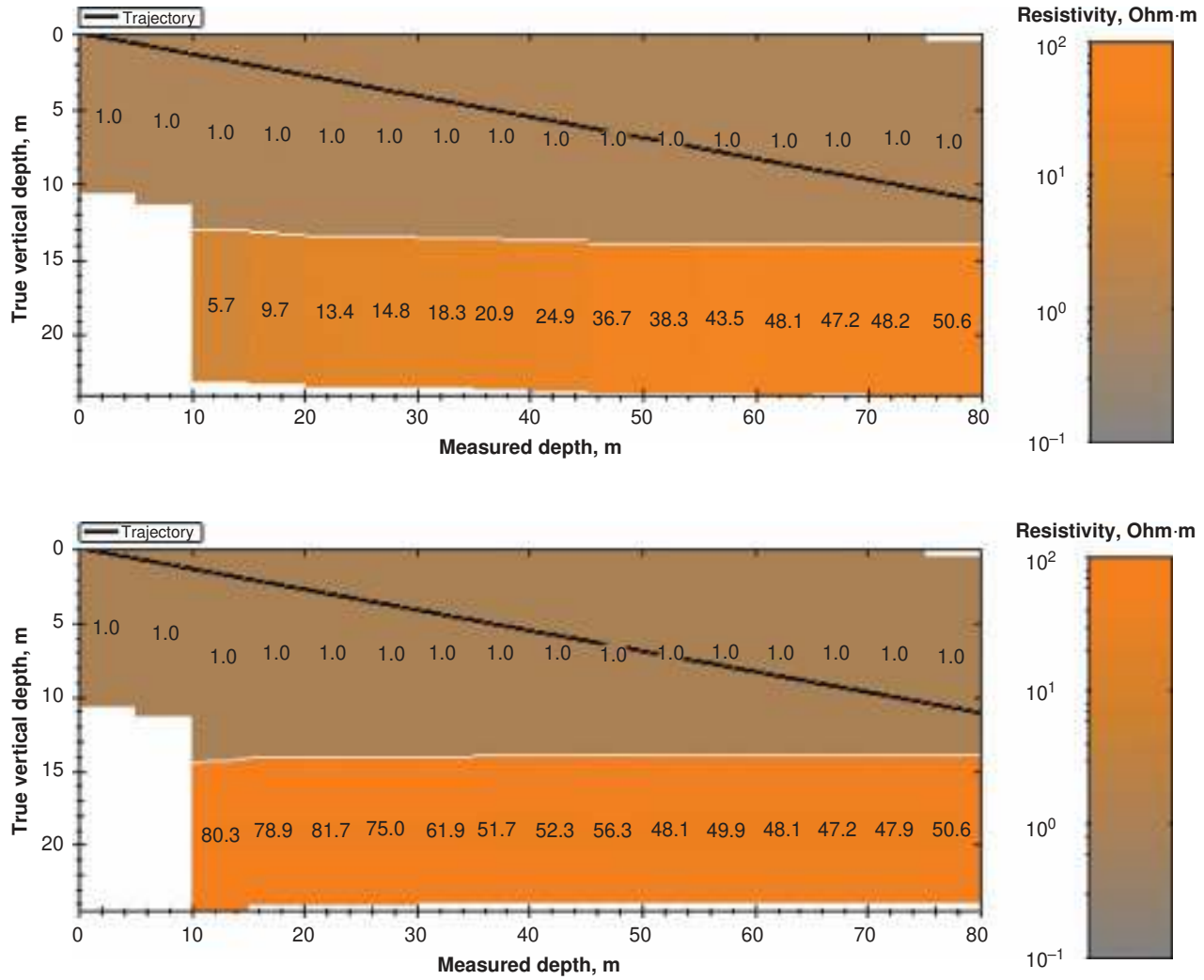

Fig. 14—(a) Model recovered by the MCWD joint inversion of extradeep and azimuthal resistivity data for the landing scenario. The *x*-axis shows the MD in meters along the borehole trajectory, which is shown as a black line. The *y*-axis shows the recovered D2B in meters in TVD. The recovered resistivity of layers for each processing window is presented in Ω·m as numbers on the plot and in corresponding colors, whereas the color-coded scheme is depicted on the right. The expected resistivity for the remote layer was set to 1 Ω·m. (b) Model recovered by the MCWD joint inversion of extradeep and azimuthal resistivity data for the landing scenario. The expected resistivity for the remote layer was set to 80 Ω·m.

presented in **Table 3.** In this case, 2-m windows were used for individual inversions. The azimuthal resistivity tool can "see" the resistive sand, starting only from the distance of approximately 2-m TVD. Close data fit for the entire interval shown in Fig. 16 confirms the high quality of inversion. It is interesting to note that no visual indications of the approaching sand are detected until 90-m MD, while the inversion enables earlier detection of the approaching bed starting from 86-m MD. Most likely, even this early detection by use of MCWD inversion would be too late for such aggressive landing with the azimuthal resistivity tool only. Considering the tool offset from the bit, the well should be drilled at a much higher angle to guarantee a smooth entrance into the reservoir.

Synthetic Example 2: Steering in a Relatively Thin Layer. Let us consider the following three-layer model (**Fig. 17**): Oil-saturated sandstone with resistivity of 50 Ω·m and a thickness of 15 m is sandwiched by 1-Ω·m shale on the top and 2-Ω·m water-saturated sand at the bottom. We assume that the well was

AQ11

TABLE 1—PARAMETER TABLE FOR THE LANDING SCENARIO BASED ON THE JOINT INVERSION OF EXTRADEEP-RESISTIVITY AND AZIMUTHAL RESISTIVITY DATA, ASSUMING THAT THE EXPECTED RESISTIVITY FOR THE REMOTE LAYER IS 1 Ω·m

Parameter; Layer No.	Resistivity, Ω·m	Anisotropy Ratio	Boundary Coordinate, m	Layer Thickness, m	Dip Angle, degrees
1	1; (0.1, 100)	1; fixed	30; (1, 30)	—	70; (60, 90)
2	1; (0.1, 100)	1; fixed	—	—	
Signals Used	Azimuthal Resistivity Tool: RA400k, RA2M, RP400k, RP2M, ImV400k Extradeep Resistivity Tool: RA20, RA50, RP20, RP50				

Each recovered parameter is characterized by expected value and ranges.
A priori known parameters are labeled as "fixed."

TABLE 2—PARAMETER TABLE FOR THE LANDING SCENARIO BASED ON THE JOINT INVERSION OF EXTRADEEP-RESISTIVITY AND AZIMUTHAL RESISTIVITY DATA, ASSUMING THAT THE EXPECTED RESISTIVITY FOR THE REMOTE LAYER IS 80 Ω·m

Parameter; Layer No.	Resistivity, Ω·m	Anisotropy Ratio	Boundary Coordinate, m	Layer Thickness, m	Dip Angle, °
1	1; (0.1, 100]	1; fixed	30; (1, 30)	—	70; (60, 90)
2	80; (0.1, 100]	1; fixed	—	—	
Signals Used	Azimuthal Resistivity Tool: RA400k, RA2M, RP400k, RP2M, ImV400k Extradeep Resistivity Tool: RA20, RA50, RP20, RP50				

Each recovered parameter is characterized by expected value and ranges.
A priori known parameters are labeled as "fixed."

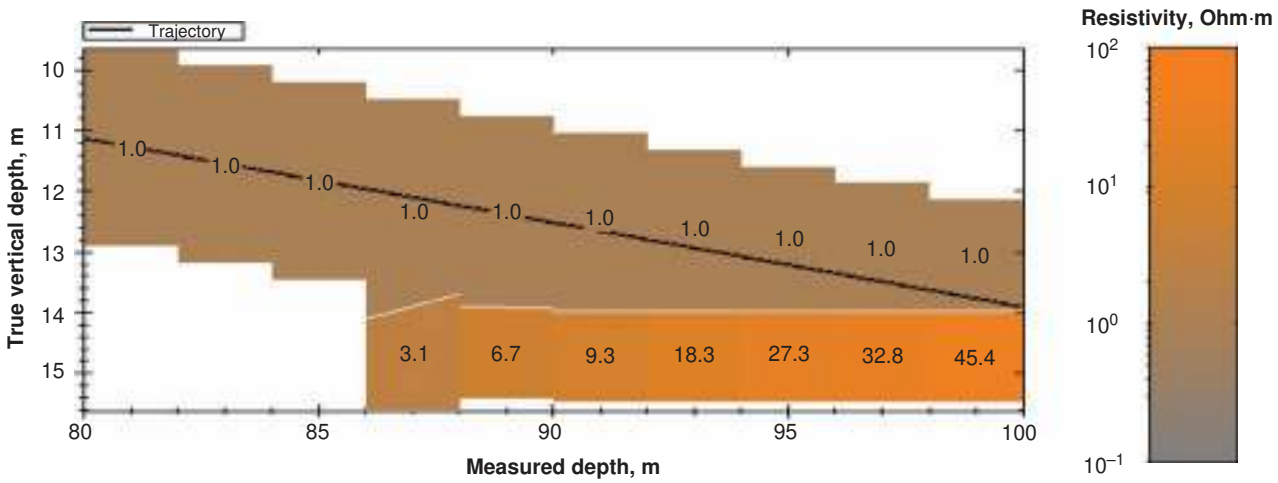

Fig. 15—Model reconstructed by the MCWD inversion for the landing scenario when only the azimuthal resistivity tool is used. The *x*-axis shows the MD in meters along the borehole trajectory, which is shown as a black line. The *y*-axis shows the recovered D2B in meters in TVD. The recovered resistivity of layers for each processing window is presented in Ω·m as numbers on the plot and in corresponding colors, whereas the color-coded scheme is depicted on the right.

successfully landed into the oil-bearing sand, and now the geosteering with respect to upper and lower boundaries should be performed. The main challenge is to stay within the reservoir—to drill out neither through the roof shale nor through the bottom-water sand. In other words, we should control the distance to upper and lower beds. We should mention that the resistivity of the upper shale and the formation dip could be constrained in the inversion processing because this information is available after the upper boundary is crossed during landing.

For simplicity, we consider the borehole trajectory placed at 85° dip and we evaluate how accurately we can resolve the distance to the upper and lower boundaries along this trajectory at the interval highlighted in blue in Fig. 17. We use 5-m-MD windows to execute inversion processing. Similar to the previous

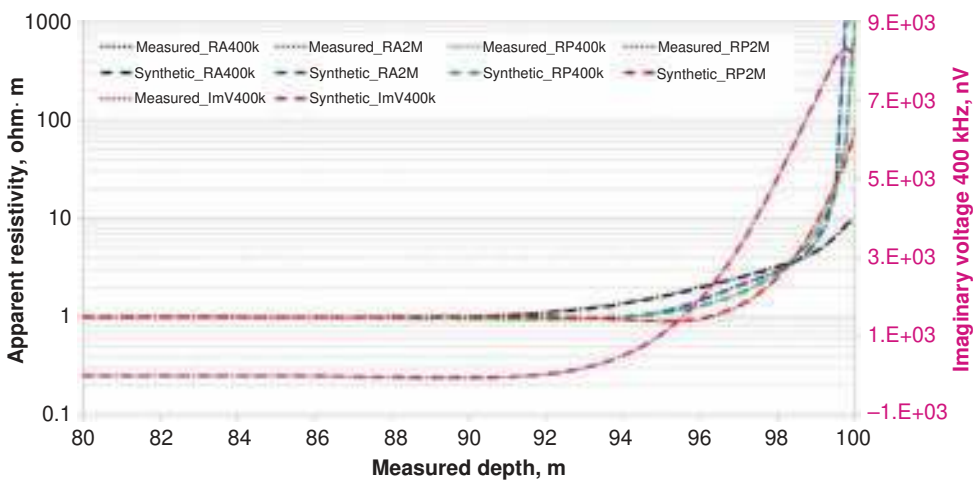

Fig. 16—Measured and synthetic signals for the landing scenario when only the azimuthal resistivity tool is used. Measured data are shown with dotted lines; calculated data for the model recovered by the inversion are shown with dashed lines. Close data fit obtained for the entire interval confirms the high quality of inversion. Visually, azimuthal resistivity data do not show any indications of the approaching sand until 90-m MD.

ID: jaganm Time: 20:12 I Path: S:/3B2/REE#/Vol00000/140009/APPFile/SA-REE#140009

TABLE 3—PARAMETER TABLE FOR THE LANDING SCENARIO WHEN ONLY THE AZIMUTHAL RESISTIVITY TOOL IS USED

Parameter; Layer No.	Resistivity, Ω·m	Anisotropy Ratio	Boundary Coordinate, m	Layer Thickness, m	Dip Angle, degrees
1	1; (0.1, 100)	1; fixed	10; (0.1, 10)	—	70; (60, 100)
2	1; (0.1, 100)	1, fixed	—	—	
Signals Used	Azimuthal Resistivity Tool: RA400k, RA2M, RP400k, RP2M, ImV400k				

Each recovered parameter is characterized by expected value and ranges.
A priori known parameters are labeled as "fixed."

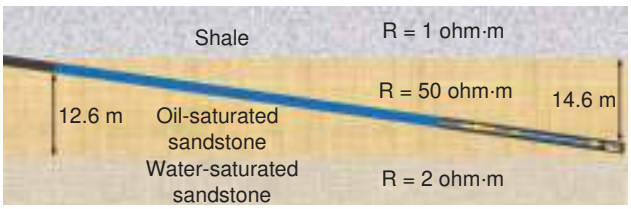

Fig. 17—Model used in Synthetic Example 2. Oil-saturated sandstone with resistivity of 50 Ω·m and a thickness of 15 m is sandwiched by 1-Ω·m shale on the top and 2-Ω·m water-saturated sand at the bottom. The well is assumed to be successfully landed into the oil-bearing sand, and geosteering with respect to upper and lower boundaries should be performed.

example, we compare steering with the combination of extradeep resistivity and azimuthal resistivity with the use of azimuthal resistivity alone. The MCWD inversion results for the combined measurements are presented in **Fig. 18.** The a priori information, initial model, and used signals are presented in **Table 4.** In this model, combining the extradeep and azimuthal resistivity measurements and the MCWD inversion enables us to determine the distances to both beds with an accuracy of ±1 m at any point along this trajectory. In addition, the resistivities of all three layers are recovered very well. These results prove that in such a model, this combination of propagation resistivity tools and the use of the MCWD inversion enables operators to geosteer successfully within the reservoir and provide maximum net pay. The operator can also take full advantage of the fact that the thickness of the layer and bed-boundary positions are determined accurately for the entire length of the borehole trajectory by use of this information for optimizing completion solutions and for reservoir modeling and management.

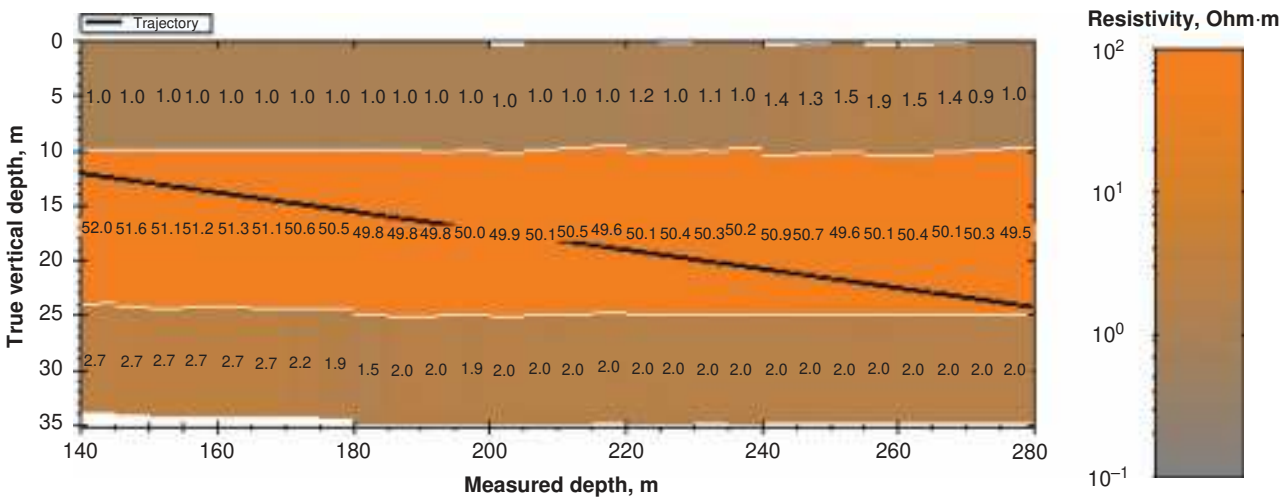

Fig. 18—Model recovered by the MCWD joint inversion of the extradeep and azimuthal resistivity data for the steering scenario. The *x*-axis shows the MD in meters along the borehole trajectory, which is shown as a black line. The *y*-axis shows the recovered D2B in meters in TVD. The recovered resistivity of layers for each processing window is presented in Ω·m as numbers on the plot and in corresponding colors, whereas the color-coded scheme is depicted on the right.

TABLE 4——PARAMETER TABLE FOR THE STEERING SCENARIO (JOINT INVERSION OF THE EXTRADEEP-RESISTIVITY AND AZIMUTHAL RESISTIVITY DATA)

Parameter; Layer No.	Resistivity, Ω·m	Anisotropy Ratio	Boundary Coordinate, m	Layer Thickness, m	Dip Angle, degrees
1	1; (0.1, 100)	1; fixed	−1; (−20, 0)	—	80; (80, 90)
2	50; (0.1, 100)	1; fixed	—	25; (0.1, 30)	
3	50; (0.1, 100)	1; fixed	—	—	
Signals Used	Azimuthal Resistivity Tool: RA400k, RA2M, RP400k, RP2M, ImV400k Extradeep Resistivity Tool: RA20, RA50, RP20, RP50				

Each recovered parameter is characterized by expected value and ranges.
A priori known parameters are labeled as "fixed."

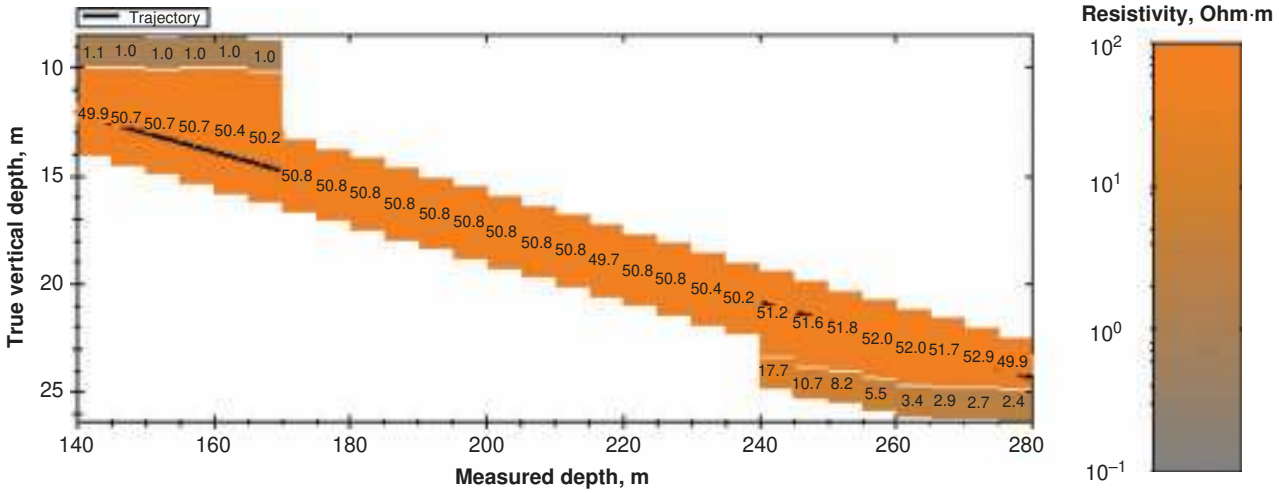

Fig. 19—Model recovered by the MCWD inversion of only the azimuthal resistivity data in the steering scenario. The *x*-axis shows the MD in meters along the borehole trajectory, which is shown as a black line. The *y*-axis shows the recovered D2B in meters in TVD. The recovered resistivity of layers for each processing window is presented in Ω·m as numbers on the plot and in corresponding colors, whereas the color-coded scheme is depicted on the right.

TABLE 5—PARAMETER TABLE FOR THE STEERING SCENARIO (INVERSION OF THE AZIMUTHAL RESISTIVITY DATA ONLY)

Parameter; Layer No.	Resistivity, Ω·m	Anisotropy Ratio	Boundary Coordinate, m	Layer Thickness, m	Dip Angle, degrees
1	1; (0.1, 100)	1; fixed	−0.5; (−5, 5)	—	80; (80, 90)
2	50; (0.1, 100)	1; fixed	—	—	
Signals Used	Azimuthal Resistivity Tool: RA400k, RA2M, RP400k, RP2M, ImV400k				

Each recovered parameter is characterized by expected value and ranges.
A priori known parameters are labeled as "fixed."

The MCWD inversion results for the azimuthal resistivity data alone are presented in **Fig. 19.** The a priori information, initial model, and used signals are presented in **Table 5.** The 5-m windows were selected for individual inversions. In this model, the azimuthal resistivity tool can "see" only one boundary at the maximum distance of approximately 4 m (this is within the tool specifications) without any chance of detecting the second boundary. Consequently, the operator must use a more cautious approach while geosteering in this reservoir, including the use of more-gentle angles. In addition, the true thickness of the reservoir will be unknown if the geosteering is performed with only the azimuthal resistivity tool.

Synthetic Example 3: Detecting a Remote Layer. The need to detect a remote resistive layer can occur in the following situations: The reservoir we are drilling in is pinching out, and its thickness became too small to justify further drilling; or the properties of the layer such as shale volume, porosity, or water saturation changed and are not good enough anymore. The latter may be identified from common neutron/density/gamma ray LWD logs that are usually run in combination with the propagation resistivity. To evaluate MCWD inversion performance by use of the combination of extradeep and azimuthal resistivity measurements, we consider the model presented in **Fig. 20.** The model consists of the upper shale layer with a resistivity of 1 Ω·m, an oil-saturated sand layer with a thickness of 20 m and a resistivity of 10 Ω·m, a screen shale layer 1 m thick with the same resistivity as the aforementioned shale, and a second productive sand layer with a resistivity of 50 Ω·m. We assume that we landed and successfully geosteered the well in the upper sand, and now we need to understand whether there is any promising object below the tool.

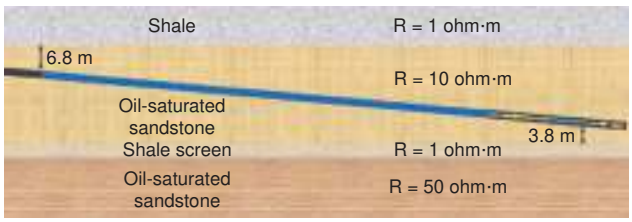

Fig. 20—Model used in Synthetic Example 3. The model consists of the upper shale layer with a resistivity of 1 Ω·m, an oil-saturated sand layer with a thickness of 20 m and a resistivity of 10 Ω·m, a 1-m-thick screen shale layer with the same resistivity as the upper shale, and a productive second sand layer with a resistivity of 50 Ω·m. The borehole is drilled at an 87° dip. While geosteering in the upper sand, we want to determine whether we can detect the resistive layer at the bottom.

Let us assume the borehole was drilled at an 87° dip. We consider a 180-m-MD interval starting at 6.8-m TVD below the upper boundary and ending at 3.8-m TVD above the thin shale layer (highlighted blue segment of borehole trajectory in Fig. 20). We use the combination of extradeep-resistivity measurements and azimuthal resistivity measurements at 10-m-MD windows to execute inversion processing. Let us assume we know the parameters of the upper shale, because we have previously drilled through that layer. This assumption means that the resistivity of the upper layer may be fixed or constrained. The MCWD inversion results for this scenario are presented in **Fig. 21;** inversion was based on a four-layer Earth model. The a priori information, initial model, and used signals are presented in **Table 6.** At the very first window, which is 13-m TVD away from the screen layer, the MCWD inversion shows the presence of another resistive layer below the shale screen. Of course, the parameters of the screen shale (its thickness and resistivity) as well as the resistivity of the bottom

ID: jaganm Time: 20:12 I Path: S:/3B2/REE#/Vol00000/140009/APPFile/SA-REE#140009

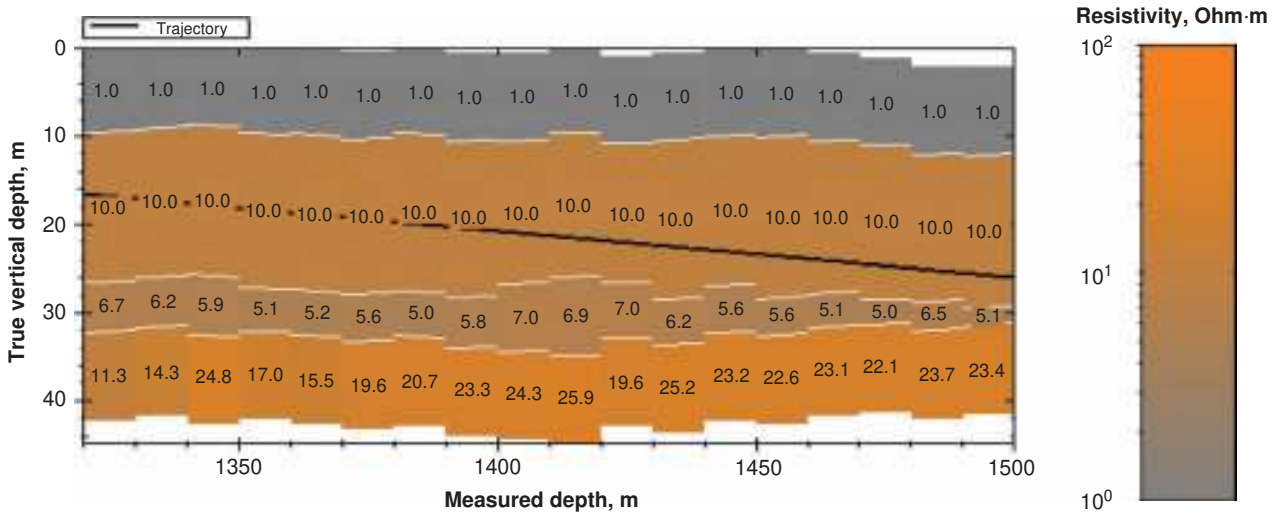

Fig. 21—Model recovered by the MCWD joint inversion of extradeep and azimuthal resistivity data for Synthetic Example 3, assuming that the inversion Earth model is consistent with the true Earth model (both models have the same number of layers). The *x*-axis shows the MD in meters along the borehole trajectory, which is shown as a black line. The *y*-axis shows the recovered D2B in meters in TVD. The recovered resistivity of layers for each processing window is presented in Ω·m as numbers on the plot and in corresponding colors, whereas the color-coded scheme is depicted on the right. The borehole trajectory is placed at 87° dip, and 10-m windows were used for individual inversions. The resistivity of the upper shale was fixed.

TABLE 6—PARAMETER TABLE FOR THE SCENARIO OF DETECTING A REMOTE RESERVOIR

Parameter; Layer No.	Resistivity, Ω·m	Anisotropy Ratio	Boundary Coordinate, m	Layer Thickness, m	Dip Angle, degrees
1	1; fixed	1; fixed	−10; (−20, −5)	—	85; (85, 90)
2	10; (1, 100)	1; fixed	—	10; (10, 30)	
3	7; (1, 8)	1; fixed	—	5; (0.5, 10)	
4	10; (8, 100)	1; fixed	—	—	
Signals Used	Azimuthal Resistivity Tool: RA400k, RA2M, RP400k, RP2M, ImV400k Extradeep Resistivity Tool: RA20, RA50,RP20, RP50				

Each recovered parameter is characterized by expected value and ranges.
A priori known parameters are labeled as "fixed."

sand are poorly resolved, but their accuracy improves when the BHA moves closer to the interface with the thin shale layer. Such an early detection of the remote resistive layer can be extremely important for an operator.

The measured and reconstructed extradeep-resistivity data for this case are presented in **Fig. 22.** The close data fit illustrates the high quality of inversion. We can notice once again that there is no chance to interpret these data with any simple visual technique.

Sometimes a misfit value obtained during inversion of real resistivity data is greater than the required threshold in the MCWD algorithm. In such cases, we can either accept the obtained model and proceed to the processing of the next data interval or add

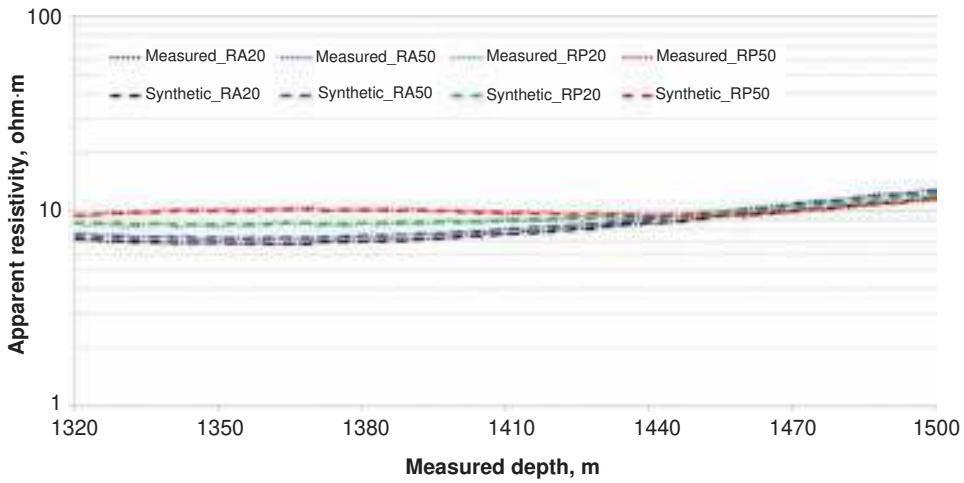

AQ8 **Fig. 22—Measured and reconstructed extradeep-resistivity signals for the scenario of detecting a remote reservoir. Measured data are shown with dotted lines; calculated data are shown with dashed lines. Close data fit is obtained along the whole interval.**

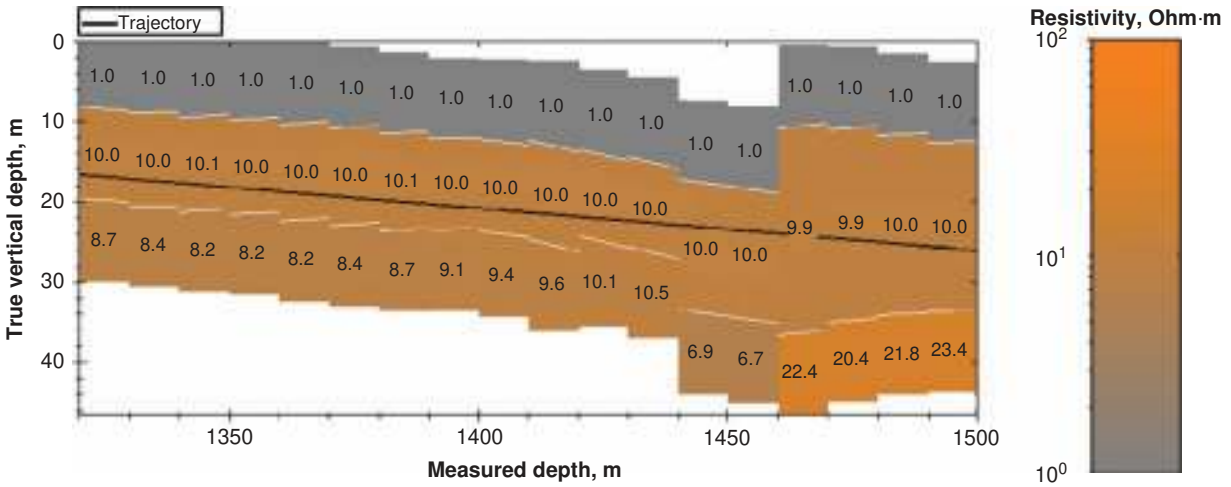

Fig. 23—Resistivity model recovered by the MCWD joint inversion of extradeep and azimuthal resistivity data for Synthetic Example 3, where the inversion Earth model was intentionally restricted by the three-layer model (inconsistent with the real four-layer Earth model). The *x*-axis shows the MD in meters along the borehole trajectory, which is shown as a black line. The *y*-axis shows the recovered D2B in meters in TVD. The recovered resistivity of layers for each processing window is presented in Ω·m as numbers on the plot and in corresponding colors, whereas the color-coded scheme is depicted on the right. The borehole trajectory is placed at 87° dip, and 10-m windows were used for individual inversions. The resistivity of the upper shale was fixed.

unknown parameters or layers into the Earth model and try to improve the data misfit with the more-complex model. Both alternatives have some inherent disadvantages. Indeed, the formation parameters recovered on the basis of the inversion model that does not describe the real medium well can be far from reality and may lead to improper geosteering decisions. For example, **Fig. 23** illustrates the MCWD inversion results for the same model presented in Fig. 20, where the inversion Earth model was intentionally restricted by the three-layer model (inconsistent with a four-layer Earth model used to generate the data). The values of recovered model parameters are not stable, and thickness of drilled reservoir and dip angle values (estimated very well in Fig. 21) are both erroneous. The a priori information, initial model, and signals used in the inversion are presented in **Table 7.**

Adding unknown parameters or layers into the inversion Earth model is not a universal panacea because high misfit value may be caused by the presence of large noise or systematic errors in measurements or caused by the inconsistency between the 1D inversion model and the real 3D geological formation. In this case, adding fictitious parameters to the inversion Earth model significantly increases the inversion ambiguity and may also result in wrong geosteering decisions. We recommend introducing additional parameters into the inversion model only if they make geological sense.

Field Case Study 1: North Sea. In this example we show the application of the MCWD inversion on azimuthal resistivity data for a well drilled in the North Sea. In this well, the azimuthal resistivity tool was used to steer a well close to the reservoir roof. A 220-ft (nearly 67-m) interval of data acquired in real time is shown in **Fig. 24.** Gamma and directional deep-resistivity images are shown in two upper tracks. The third track from the top displays azimuthal signals from 16 sectors ("jellyfish" curves), and the bottom track depicts four conventional propagation resistivity curves. The azimuthal signal strength curve in red (Sector 0) corresponds to the tool face pointing up and clearly shows excessive conductivity above the tool. Increase in this signal in the interval X050–X190 ft clearly indicates that the tool is gradually approaching the reservoir roof. This is consistent with conventional resistivity curves' separation in the bottom track. The shallowest curve (2-MHz Phase, in red) reads high resistivity values in sand, whereas the deepest curve (400-KHz Attenuation, in black) decreases as more-conductive shale volume is included in the tool sensitivity range.

A shale injectile is crossed at X195–X225-ft MD, as shown by gamma ray image and resistivity logs. The shallowest 2-MHz phase resistivity (red curve) reads approximately 5–10 Ω·m inside that interval and above 100 Ω·m everywhere else.

We applied the MCWD inversion during a post-drill analysis to obtain a quantitative estimation of D2B, relative dip, and formation resistivities. The interval was split into several processing windows. The windows were shorter for the conductive segment because the injectile was detected there and a horizontally layered model in the bigger windows was not suitable anymore. Seven curves, including six apparent resistivities and one azimuthal voltage, were jointly processed in each window and merged into one image presented in **Fig. 25.** The a priori information, initial

AQ3

AQ12

TABLE 7—PARAMETER TABLE FOR THE SCENARIO OF DETECTING A REMOTE RESERVOIR WHERE INVERSION EARTH MODEL WAS INTENTIONALLY RESTRICTED BY THE THREE-LAYER MODEL (INCONSISTENT WITH THE REAL FOUR-LAYER EARTH MODEL)

Parameter; Layer No.	Resistivity, Ω·m	Anisotropy Ratio	Boundary Coordinate, m	Layer Thickness, m	Dip Angle, degrees
1	1; fixed	1; fixed	−10; (−30, 0)	—	90; (70, 110)
2	30; (0.1, 100)	1; fixed	—	30; (0.1, 30)	
3	30; (0.1, 100)	1; fixed	—	—	
Signals Used	Azimuthal Resistivity Tool: RA400k, RA2M, RP400k, RP2M, ImV400k Extradeep Resistivity Tool: RA20, RA50,RP20, RP50				

Each recovered parameter is characterized by expected value and ranges.
A priori known parameters are labeled as "fixed."

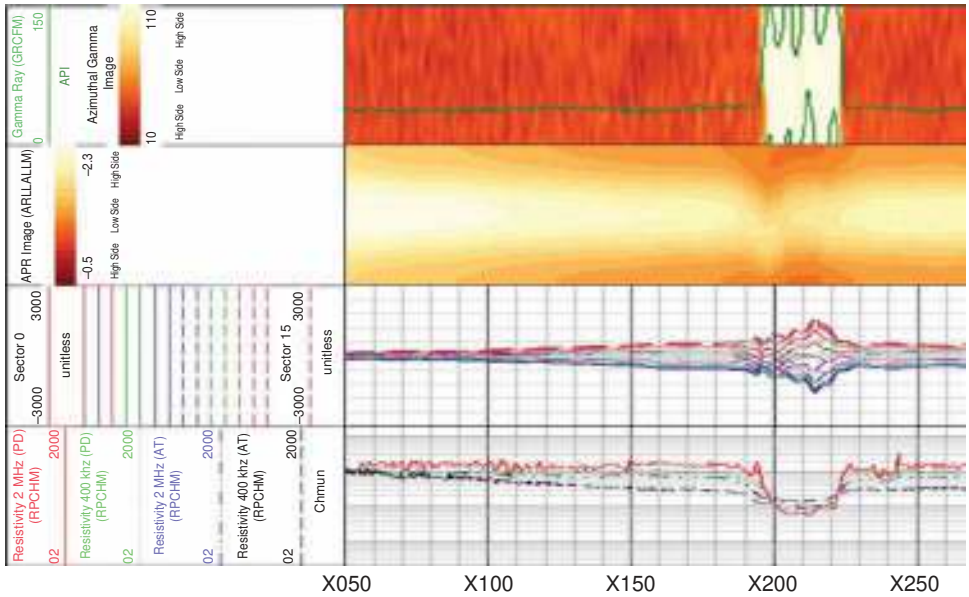

Fig. 24—Logging data for the North Sea case study on the interval X050–X270 ft. Gamma ray curve in green and azimuthal Gamma image is shown in the upper track. Directional deep-resistivity image is presented on the second track from the top. The third track from the top displays azimuthal signals from 16 sectors. The bottom track depicts four conventional propagation resistivity curves.

model, and signals used in the inversion are presented in **Table 8.** A two-layer model appeared to be satisfactory in the MCWD inversion, and the following parameters were determined: Upper layer was anisotropic with $R_h = 3$–3.5 Ω·m and an anisotropy coefficient of 1.4 to 1.7. The lower layer is isotropic; its resistivity varies from 160 to 190 Ω·m. Data match is shown in **Fig. 26.**

The MCWD inversion results presented in Fig. 25 clearly show the shale injectile on the interval X190–X220 ft and determine its parameters. The data match is not very good in that interval because the 1D horizontally layered model does not adequately represent the real geological situation. In addition, horn effects are observed in the data where the tool enters and exits the injectile.

We should mention that the main goal of geosteering with the azimuthal resistivity tool is to avoid drilling into a conductive layer. In the situation described here, the injectile could not be avoided because it came at a high apparent angle. In such cases, the extradeep-resistivity tools and more-complicated inversion models are needed.

Field Case Study 2: GOM. Fig. 27 shows azimuthal gamma ray and azimuthal resistivity data in formation structure drilled downward in a GOM well. Several layers are crossed, as indicated in images and resistivity tracks. The azimuthal resistivity signal corresponding to the tool face (red curve on the third track from the top) is negative when a more conductive layer is below the tool, and becomes positive after the tool is underneath the layer (interval Y700–Y800 ft). On the last 150 ft of the log, the azimuthal signal shows the tool is approaching two conductive layers, and

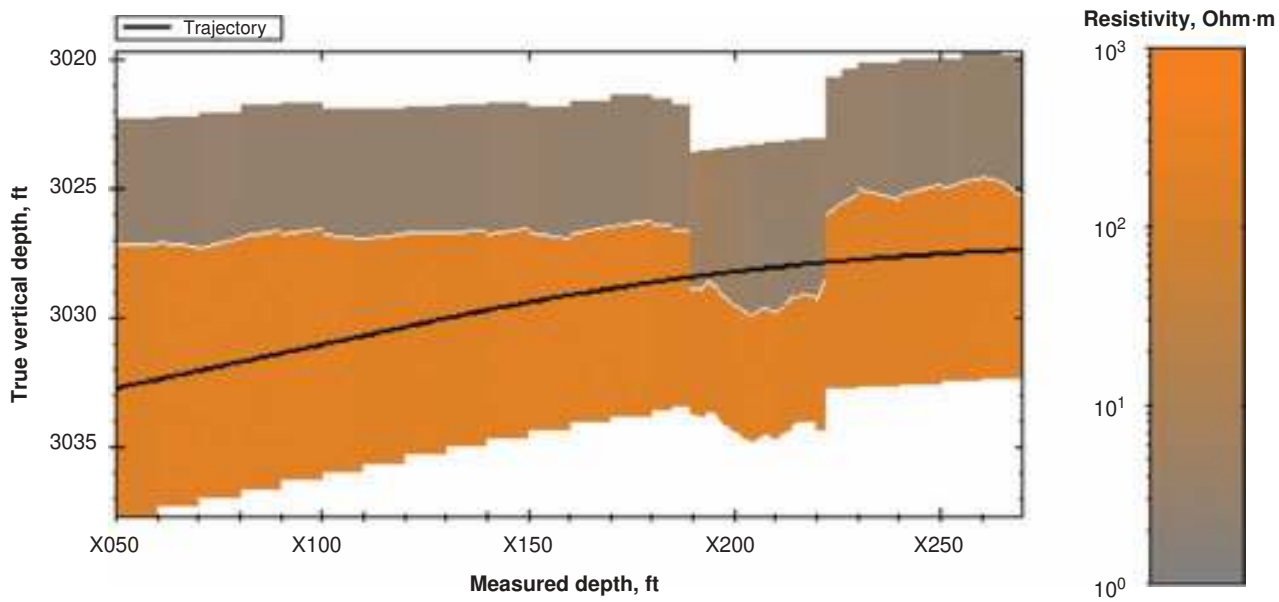

Fig. 25—Model reconstructed by the MCWD along the interval X050–X270 ft. The recovered resistivity is presented in a color-coded scheme depicted on the right. The borehole trajectory is shown as a black solid line. A shale injectile is observed on the interval X190–X220 ft. A 1D model with two layers is suitable for the whole interval except sections where the well enters and exits the injectile, for which a more complicated model is required.

ID: jaganm Time: 20:12 I Path: S:/3B2/REE#/Vol00000/140009/APPFile/SA-REE#140009

AQ13

TABLE 8—PARAMETER TABLE FOR THE NORTH SEA CASE STUDY

Parameter; Layer No.	Resistivity, Ω·m	Anisotropy Ratio	Boundary Coordinate, m	Layer Thickness, m	Dip Angle, degrees
1	3.25; (3, 10)	1.5; (1, 3)	−1; (−3, 3)	—	93; (75, 110)
2	175; (160, 190)	1, fixed	—	—	
Signals Used	Azimuthal Resistivity Tool: RAS400k, RPS400k, RA400k, RA2M, RP400k, RP2M, ImV400k				

Each recovered parameter is characterized by expected value and ranges.
A priori known parameters are labeled as "fixed."

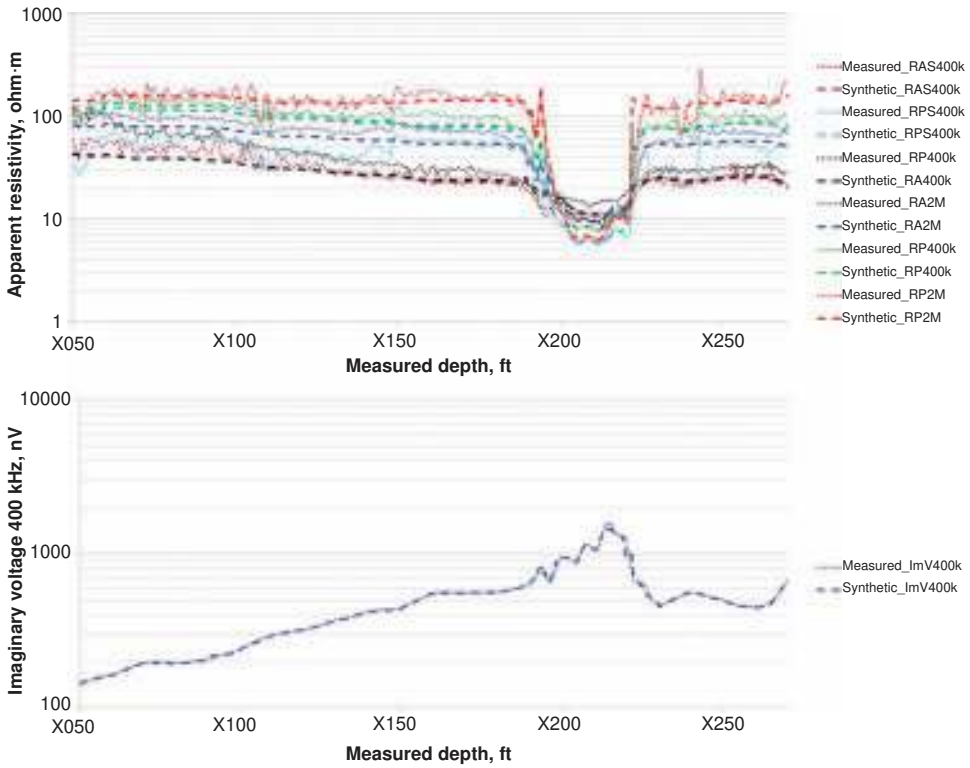

Fig. 26—Measured and simulated data for the North Sea case study. The upper plot shows six omnidirectional resistivities. The bottom plot displays azimuthal voltage. Measured data are shown with dotted lines; calculated data are shown with dashed lines. Good data fit is reached for the entire interval except sections where the well enters and exits the injectile. In these sections, the horn effects are present in the data and the 1D interpretation model is inadequate.

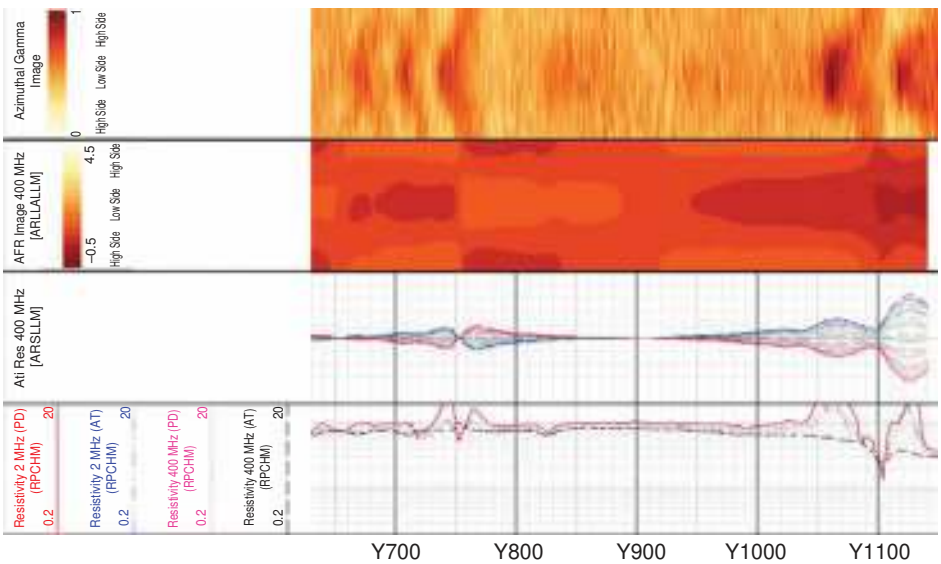

AQ9

Fig. 27—Crossing thin layers in the GOM case study. Data presented on tracks (top to bottom): gamma ray image, azimuthal resistivity image, azimuthal resistivity 16-sector curves, and propagation resistivity.

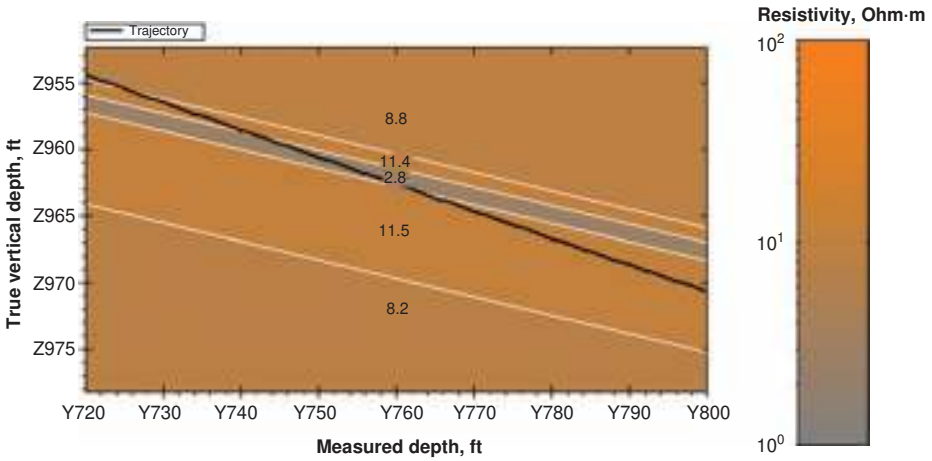

Fig. 28—Model reconstructed on 80-ft interval when tool crossed thin shale. The recovered resistivity of layers is presented in Ω·m as numbers on the plot and in corresponding colors, whereas the color-coded scheme is depicted on the right. The whole interval was processed at once.

while crossing several boundaries, it always shows excessive conductivity below. Because only the azimuthal resistivity tool was used for geosteering in this well (RA400k, RA2M, RP400k, RP2M, and ImV400k signals), and the geology penetrated by the well is not simple, there are not enough independent real-time measurements to reliably resolve all the parameters of the thin layers by use of short inversion windows. To make the results of inversion more stable, the longer intervals were chosen for processing.

The first interval, Y720–Y800 ft, was processed by the MCWD inversion by use of a model with five layers. The match of the measured and synthetic data was quite good for the whole interval. The resulting model is shown in **Fig. 28.** The inversion reliably identified thin conductive shale and its parameters.

AQ4 The second interval, Y1000–Y1150 ft, covers the last part of the well exiting from sand and TD in shale **(Fig. 29).** The underlying model for inversion contained seven layers. Parameters of the top three layers were restricted on the basis of results from the previous interval, but not fixed. Although the software is capable of fixing the parameters of layers that have already been crossed by the borehole, we did not do it here. Thus, for relatively remote layers, an equivalent model often can be found. Similar to upper shale, the middle sand represented in the first interval by two layers (where lower layer has slightly decreased resistivity of 8.2 Ω·m, reflecting presence of shale below) is approximated on the second interval by one layer with averaged resistivity. Varying parameters of the remaining layers intersected by the wellbore enabled the data fitting on this interval reasonably well. The main purpose of this case study was to demonstrate multiboundary AQ5 inversion on relatively long log intervals with rich curve features. We should note that although in Fig. 29 we show the bottom shale AQ6 as infinite, in reality we do not know its thickness because the DOI of the azimuthal propagation tool is very limited in conductive formations.

Conclusions

We have developed an efficient algorithm and flexible, user-friendly MCWD software for reservoir-navigation applications. The MCWD software can perform real-time processing of any combination of the omnidirectional, azimuthal, and extradeep LWD resistivity measurements. The algorithm is based on a 1D anisotropic layered model with an arbitrary number of layers, and any parameters of this model and a tool position relative to layer boundaries can be recovered. The software has been used for real-time landing and geosteering applications and for post-drill analysis, providing accurate estimates of formation parameters critical for formation evaluation, completion decisions, reservoir modeling, and reservoir management. Application of the developed software has been shown on a series of synthetic examples and field data from the North Sea and from the GOM.

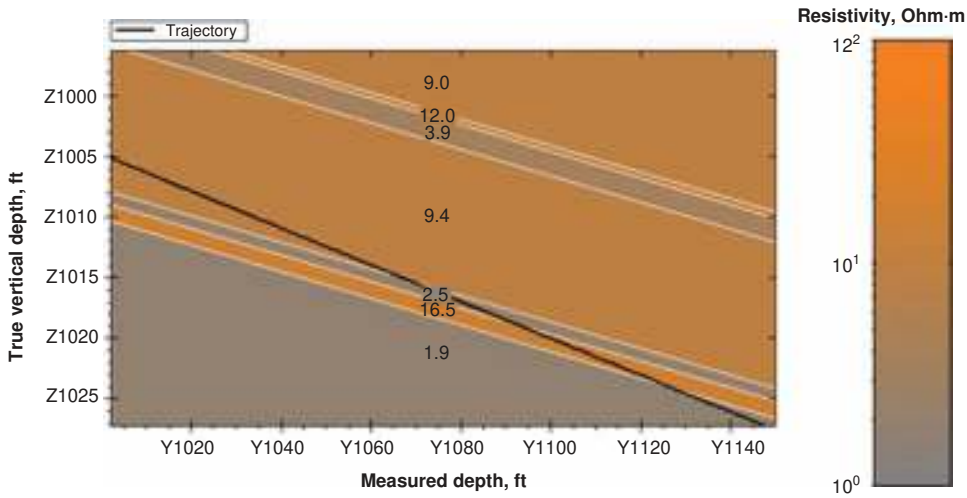

Fig. 29—Model reconstructed by the MCWD inversion for the 150-ft interval with well exiting sand. The recovered resistivity of layers is presented in Ω·m as numbers on the plot and in corresponding colors, whereas the color-coded scheme is depicted on the right.

AQ7

Nomenclature

ImV2M = azimuthal signal strength, imaginary voltage for the 2-MHz (ZX signal), for the azimuthal resistivity tool
ImV400k = azimuthal signal strength, imaginary voltage for the 400-kHz (ZX signal), for the azimuthal resistivity tool
RA20 = attenuation apparent resistivity for the 20-kHz (ZZ signal), for the extradeep-resistivity tool
RA2M = attenuation apparent resistivity for the 2-MHz long-spaced array (ZZ signal), for the azimuthal resistivity tool
RA50 = attenuation apparent resistivity for the 50-kHz (ZZ signal), for the extradeep-resistivity tool
RA400k = attenuation apparent resistivity for the 400-kHz long-spaced array (ZZ signal), for the azimuthal resistivity tool
RAS400k = attenuation apparent resistivity for the 400-kHz short-spaced array (ZZ signal), for the azimuthal resistivity tool
RP20 = phase difference apparent resistivity for the 20-kHz (ZZ signal), for the extradeep-resistivity tool
RP2M = phase difference apparent resistivity for the 2-MHz long-spaced array (ZZ signal), for the azimuthal resistivity tool
RP50 = phase difference apparent resistivity for the 50-kHz (ZZ signal), for the extradeep-resistivity tool
RP400k = phase difference apparent resistivity for the 400-kHz long-spaced array (ZZ signal), for the azimuthal resistivity tool
RPS400k = phase difference apparent resistivity for the 400-kHz short-spaced array (ZZ signal), for the azimuthal resistivity tool

Acknowledgments

The authors wish to thank Chevron and BP for the release of the field data. We also want to thank Baker Hughes and BP for permission to publish the paper. The authors appreciate the efforts of our colleagues S. Terentyev, V. Mogilatov, T. Eltsov, and E. Vtorushin, who contributed to the algorithm and software development at different stages of this project. We are grateful to the members of the Resistivity Interpretation and Reservoir Navigation teams for fruitful discussions and helpful suggestions, and in particular to R. Tilsley-Baker for testing the MCWD software. Special thanks to N.F. Atzmiller and L. Johnson for reviewing the paper.

References

Dennis, J. E. and Schnabel, R. B. 1988. *Numerical Methods for Unconstrained Optimization and Nonlinear Equations*. Moscow, USSR: Mir Publishers.

Fang, S., Merchant, A., Hart, E., et al. 2008. Determination of Structural Dip and Azimuth from LWD Azimuthal Propagation Resistivity Measurements in Anisotropic Formations. Paper SPE 116123 presented at 2008 SPE Annual Technical Conference and Exhibition, Denver, Colorado, 21–24 September. http://dx.doi.org/10.2118/116123-MS.

Gill, P. E. and Murrey, W. 1977. *Numerical Methods for Constrained Optimization*. Moscow, USSR: Mir Publishers.

Helgesen, T. B., Meyer, W. H., Thorsen, A. K., et al. 2004. Accurate Wellbore Placement Using a Novel Extra Deep-Resistivity Service. Paper SPE 94378 presented at the SPE Europec/EAGE Annual Conference, Madrid, Spain, 13–16 June. http://dx.doi.org/10.2118/94378-MS.

Himmelblau, D. 1975. *Applied Nonlinear Programming*. Moscow, USSR: Mir Publishers.

Moré, J. J and Sorensen, D. C. 1983. Computing a Trust Region Step. *SIAM J. Sci. Stat. Comp.* **4** (3): 553–572. http://dx.doi.org/10.1137/0904038.

Pardalos, P. M. and Romeijn, H. F. 2002. *Handbook of Global Optimization*, Vol. 2. Dordrecht, Netherlands: Kluwer.

Pustilnik, E. I. 1968. *Statistical Methods of Data Analyze and Processing*. Moscow, USSR: Nauka.

Rabinovich, M., Le, F., Lofts, J., et al. 2011. The Vagaries and Myths of Look-Around Deep-Resistivity Measurements While Drilling. Oral presentation given at the Society of Petrophysicists and Well Log Analysts (SPWLA) 52nd Annual Logging Symposium, Colorado Springs, Colorado, 14–18 May.

Seydoux, J., Tabanou, J., Ortenzi, L., et al. 2003. A Deep-Resistivity Logging-While-Drilling Device for Proactive Geosteering. Paper OTC 15126 presented at the Offshore Technology Conference, Houston, Texas, 5–8 May. http://dx.doi.org/10.4043/15126-MS.

Stone, M. 1974. Cross-Validatory Choice and Assessment of Statistical Predictions. *J. Roy. Stat. Soc. B. Met.* **36** (2): 111–147. http://www.jstor.org/stable/2984809.

Tikhonov, A. N. and Arsenin, V. J. 1979. *Methods of Solving Ill-Posed Problems*. Moscow, USSR: Nauka.

Verlan, A. F. and Sizikov, V. S. 1986. *Integral Equations: Methods, Algorithms, Codes*. Kiev, USSR: Naukova Dumka.

Wang, T., Chemali, R., Hart, E., et al. 2007. Real-Time Formation Imaging, Dip, And Azimuth While Drilling From Compensated Deep Directional Resistivity. Paper SPWLA 2007_NNN presented at the 48th SPWLA Annual Logging Symposium, Austin, Texas, 3–6 June.

Yanovskaya, T. B. and Porokhova, L. N. 1983. *Inverse Problems in Geophysics*. Leningrad, USSR: Leningrad State University Press.

Mikhail Sviridov holds a master's degree in applied mathematics and informatics from Novosibirsk State University, Russia. He joined the Baker Hughes Novosibirsk Technology Center in 2008 as a scientist. Sviridov's research interests include numerical methods for modeling and inversion in geophysics. He is currently involved in the development of interpretation software for LWD resistivity tools.

Anton Mosin holds a master's degree in applied mathematics and informatics from Novosibirsk State University. He has worked as a scientist for Baker Hughes since 2008. Mosin's research interests include numerical methods for modeling and inversion of electromagnetic geophysical data and enterprise software development. He is currently involved in the development of software for proactive geosteering.

Yuriy Antonov holds master's and PhD degrees in geophysics from Novosibirsk State University and the Russian Academy of Science, respectively. He has worked for Baker Hughes since 2008 as a scientist. Antonov participated in the development of the processing software for wireline and LWD resistivity tools. He is a coauthor of five publications.

Marina Nikitenko holds a master's degree in mathematics from the Novosibirsk State University and a PhD degree in technical sciences from the Russian Academy of Science. From 1985 to 1991, she worked at SibOilGeophysics as an engineer. In 1991, Nikitenko moved to the Institute of Petroleum Geology and Geophysics of the Siberian Branch of the Russian Academy of Science, where she continues to work as a senior scientist. Since 2005, Nikitenko has worked as a senior geoscientist at Baker Hughes Novosibirsk Technology Center. Her research interests include solving forward and inverse problems of electromagnetic well logging. Nikitenko is currently involved in the development of resistivity interpretation software including modeling, sensitivity analysis, and inversion. She is the author/coauthor of approximately 50 publications (mainly in Russia) and holds two patents.

Sergey Martakov holds a master's degree from Novosibirsk State University and a PhD degree from the Russian Academy of Sciences, both in mathematics. Markatov's interests include numerical methods for modeling and inversion in geophysical and other applications, as well as research and enterprise software development. Since 2008, he has worked at the Baker Hughes Houston Technology Center as a senior scientist.

Michael B. Rabinovich holds a master's degree from Moscow Institute of Oil and Gas Industry and a PhD degree from the Russian Academy of Science, both in geophysics. From 1994 to 2011, he worked as a research and senior scientist and a

Deputy Director for Drilling & Evaluation Research with Baker Hughes in Houston. Rabinovich participated in the development of the processing and interpretation software for all modern wireline and LWD resistivity tools. Since February 2012, he has worked at BP as a subject-matter expert in resistivity and electromagnetic-log measurements, providing consultancy support to BP's assets around the world in tool technology selection, interpretation, and geosteering applications. Rabinovich is the author/coauthor of more than 80 publications and holds 44 patents.

Author Queries

AQ1: Changed Helgesen et al. 2005 to Helgesen et al. 2004 to match the reference list. If not as meant, please revise here and in the reference list.

AQ2: Authors, can you list the terms along with describing them as “first term,” “second term,” and “third term” for clarity purposes? Please advise.

AQ3: Authors, should this be gamma ray, not gamma? Please advise.

AQ4: Authors, is this “TD” meant to be short for total depth? Or is “TD” a typo for “TVD”? Please advise.

AQ5: Changed “The main purpose of this example” to “The main purpose of this case study”. If not as meant, please revise.

AQ6: Changed reference to figure 28 to reference to figure 29. If not as meant, please revise.

AQ7: Authors, please define the other symbols used in the article in this section, including those used in the equation and any others throughout the text. The list should include the letter symbol, an accurate and concise definition, the dimensions in which the quantity is measured, and the units of measure used in the paper.

AQ8: Changed synthetic to reconstructed in the legend for figure 22 to match the text. If not as meant, please revise and check the text.

AQ9: Please verify renumbering of figure legends is correct.

AQ10: ED: Please check dates for the review process. They appear out of order.

AQ11: Kristin, all mentions of “ohm.m” in the text and tables have been changed to “Ω·m,” which I did because of the style guide.

AQ12: Previously Table 6a, now Table 7.

AQ13: Previously Table 7, now Table 8.